
Palaeoproterozoic adakite- and TTG-like magmatism in the Svecofennian orogen, SW Finland

M. VÄISÄNEN^{1,*} | Å. JOHANSSON² | U.B. ANDERSSON³ | O. EKLUND⁴ | P. HÖLTTÄ⁵

¹ | Department of Geography and Geology, University of Turku
FI-20014 Turku, Finland. E-mail: markku.vaisanen@utu.fi

² | Laboratory for Isotope Geology, Swedish Museum of Natural History
Box 50007, SE-104 05 Stockholm, Sweden. E-mail: ake.johansson@nrm.se

³ | Department of Earth Sciences, Uppsala University
Villavägen 16, SE-752 36 Uppsala, Sweden. E-mail: ulf.andersson@nrm.se

⁴ | Department of Geology and Mineralogy, Åbo Akademi University
FI-20500 Turku, Finland. E-mail: olav eklund@abo.fi

⁵ | Geological Survey of Finland GTK
P.O. Box 96, FI-02151 Espoo, Finland. E-mail: pentti.holtt@gtk.fi

* Corresponding author

ABSTRACT

The Palaeoproterozoic Svecofennian orogen in the Fennoscandian shield is an arc accretionary orogen that was formed at *c.* 1.92-1.86Ga. Arc accretion, magmatism and the subsequent continent-continent collision thickened the crust up to *c.* 70km, forming one of the thickest Palaeoproterozoic orogens. At the end stage of accretionary tectonics, voluminous synorogenic magmatism occurred in southwestern Finland leading to the intrusion of intermediate to felsic plutonic rocks. Ion microprobe single zircon dating of one diorite sample yielded an age of 1872±3Ma ($\epsilon_{Nd}=+2.2$) and the trondhjemite sample an age of 1867±4Ma ($\epsilon_{Nd}=+2.6$). Inherited 2667-1965Ma cores and 1842±5Ma metamorphic rims were also found in zircons from the trondhjemite.

The dioritic magmatism is mantle-derived and is slightly enriched by subduction-related processes. The felsic magmatism shows elevated Sr/Y and La/Yb ratios, which are typical for adakite- and TTG-like magmas. Their low Mg#, Ni and Cr contents argue against slab-melting and mantle-wedge contamination. We infer that the felsic magmatism was generated through crustal melting of the lower part of the previously generated volcanic-arc type crust. Based on published melting experiments and the Sr and Y contents of the felsic rocks we suggest that the melts were generated at a minimum pressure of 10kbar, with evidence of a 15kbar pressure for the highest Sr/Y trondhjemites. It is proposed that arc accretion combined with magmatic intrusions thickened the crust so that melting of the lower crust yielded adakite- and TTG-like compositions. The mafic magmatism is considered to be the heat source.

KEYWORDS | Adakite. TTG. Palaeoproterozoic. Svecofennian. U-Pb. Sm-Nd. SIMS. Diorite. Tonalite. Trondhjemite. Granodiorite. Crustal melting.

INTRODUCTION

Adakites have recently been widely discussed because of their specific composition that reflects their source region and indirectly gives hints of their tectonic setting. Adakitic magmas were originally regarded to have formed by melting of subducted oceanic slabs, and contaminated by mantle-wedge peridotite during ascent, forming a minor part of modern volcanic arc rocks (Defant and Drummond, 1990). Recently, however, it has been shown that magmas with the characteristically high Sr/Y and La/Yb ratios, the most common geochemical discriminants for adakites, can be produced in many different ways, where slab melting is only one of them. Therefore, some authors warn against the uncritical use of such geochemical signatures for adakites, especially if used in a petrogenetic or tectonic sense (*e.g.*, Richards and Kerrich, 2007; Moyen, 2009). If strictly adhering to the definitions of adakites (Defant and Drummond, 1990; Martin, 1999; Martin *et al.*, 2005; Richards and Kerrich, 2007), at least the high-silica adakites (HSA) show evidence of slab melting (Martin *et al.*, 2005). Adakitic compositions can in most cases be regarded as evidence of high pressure melting of garnet-bearing mafic sources, where garnet remains in the residue (low HREE and Y in the melt) and plagioclase goes into the melt (high Sr). Medium pressure melting of garnet-bearing pelitic rocks may also lead to high La/Yb, but in those cases other geochemical features would not be adakitic (Moyen, 2009). In addition, crustal assimilation and fractionation processes can in some cases produce adakitic compositions (*e.g.*, Macpherson *et al.*, 2006). It is seldom that all samples and elements of the studied rocks match the adakitic definitions, but instead show some deviation. Such rocks are often referred to as adakite-like rocks (*e.g.*, Richards and Kerrich, 2007).

Archaean tonalite-trondhjemite-granodiorite (TTG; Jahn *et al.*, 1981) series rocks share many characteristics with modern adakites. Therefore, it has been argued that Archaean high-Al TTG series rocks are analogues of modern adakites, and were formed in a similar tectonic setting, *i.e.* through melting of subducted oceanic crust (Martin, 1999). In fact, most major and trace element characteristics of adakites and TTGs are strikingly similar, indicating a similar origin (Martin *et al.*, 2005). However, in detail, TTGs often have a higher silica content and a lower magnesium number (Mg#) and Sr, Ni and Cr contents. This has been interpreted by some authors to show that TTGs never interacted with mantle wedge peridotite and therefore cannot be slab melts (*e.g.*, Smithies, 2000; Kamber *et al.*, 2002; Condie, 2005).

Palaeoproterozoic adakites have been very rarely described, at least using the term adakite. In fact, we have found only two examples in the literature: 1.85Ga crustally derived adakites from Australia (Shepard *et al.*, 2001) and

2.17-2.13Ga adakites from Brazil (Martins *et al.*, 2009). In spite of being abundant in the earliest Earth history, TTGs are found throughout geological time (Condie, 2005). One problem with TTGs seems to be that no consensus has been reached on how to exactly define them (*c.f.*, Smithies, 2000; Condie, 2005; Martin *et al.*, 2005). As a result, rocks with closely similar compositions have been classified as TTG, adakite, or just using rock names such as quartz-diorite, tonalite, trondhjemite or granodiorite. Recently, however, TTGs have also been classified in more detail (*e.g.*, Halla *et al.*, 2009). When TTGs are found in rocks younger than Archaean, they are sometimes referred to as TTG-like (*e.g.* Zhang *et al.*, 2009).

In this article we describe and discuss the origin of synorogenic plutonic rocks from the Palaeoproterozoic Svecofennian orogen in southwestern Finland, which have compositions that straddle those described as adakites and TTGs, to place constraints on the geodynamic process leading to the formation of these rocks. Apart from whole rock chemical analyses, we present single zircon U-Pb ion microprobe age determinations and Sm-Nd isotopes on one diorite and one trondhjemite sample. The main geochemical constraints defining adakites and TTGs (in brackets) are adopted from Defant and Drummond (1990) and Martin *et al.* (2005): SiO₂ (wt. %) >56 (>64); Mg# ~51 (~43); Ni (ppm) ~24 (~14); Cr (ppm) ~36 (~29); Sr (ppm) >400 (>400); Y (ppm) ≤ 18 (<15); Yb (ppm) ≤ 1.9 (<1.6); Sr/Y >40 (>40); La/Yb >20 and (La/Yb)_N >10. Other criteria are explained in the figures and text. We use here the terms adakite- and TTG-like only as compositional terms, without any primary reference to age or tectonic setting.

GEOLOGICAL FRAMEWORK

The Palaeoproterozoic Svecofennian orogen (Fig. 1) is traditionally classified as an arc-accretionary orogen (Windley, 1995) in which several volcanic arc complexes (terrane) have been successively accreted to the Archaean Karelian craton in the present northeast to form the Svecofennian domain (Gaál and Gorbatshev, 1987; Lahtinen, 1994; Nironen, 1997; Korsman *et al.*, 1999; Vaasjoki *et al.*, 2003; Mansfeld *et al.*, 2005). This concept has been challenged by Rutland *et al.* (2004) and Williams *et al.* (2008) who interpret the Svecofennian domain as a marginal basin sequence intruded by igneous complexes.

Present models (*e.g.*, Lahtinen *et al.*, 2005; Korja *et al.*, 2006) subdivide the Svecofennian orogeny in southern Finland into four major stages: i) formation and accretion of arc terranes at 1.92-1.87Ga, ii) extension of accreted terranes at 1.86-1.84Ga, iii) continental collision at 1.84-1.79Ga, iv) and finally a gravitational collapse of the thickened orogen at 1.79-1.77Ga. These processes partly

overlapped in time in different parts of the Domain (Korja *et al.*, 2006). The accreted terranes probably include older unexposed *c.* 2.1-1.93Ga crustal fragments, as indicated by weakly depleted to chondritic initial ϵ_{Nd} and ϵ_{Hf} values (Patchett *et al.*, 1987; Huhma, 1986; Valbracht *et al.*, 1994; Lahtinen and Huhma, 1997; Rämö *et al.*, 2001; Andersen *et al.*, 2009), as well as detrital zircons in metasediments and inherited zircons in igneous rocks (*e.g.*, Claesson *et al.*, 1993; Lahtinen *et al.*, 2002, 2009; Ehlers *et al.*, 2004; Andersson *et al.*, 2006b; Bergman *et al.*, 2008). In addition, the volcanic rocks commonly have continental margin or rifting type lithological associations and geochemical affinities (*e.g.*, Baker *et al.*, 1988; Allen *et al.*, 1996; Kähkönen, 2005; Weihed *et al.*, 2005), indicating the existence of hidden older crust beneath or adjacent to the present one. Recent palaeotectonic models emphasize the importance of post-accretional continent-continent collisions with Sarmatia and possibly also with Amazonia (Lahtinen *et al.*, 2005; Bogdanova *et al.*, 2008; Johansson, 2009), as well as continued convergence at an active continental margin in the SW (Andersson *et al.*, 2004b, 2007; Rutanen and Andersson, 2009).

The southern Svecofennian arc complex (Fig. 1B) in southern Finland is a terrane that includes two volcanic belts; the Uusimaa belt and the Häme belt, where volcanic rocks have been dated at 1.90-1.88Ga (Kähkönen, 2005 and references therein). These volcanic belts are closely associated with sedimentary rocks that were deposited in basins formed by extension of the volcanic arcs. Tholeiitic mafic and ultramafic volcanic rocks were also extruded in these extensional basins (Ehlers *et al.*, 1986; Väisänen and

Mänttari, 2002; Ogenhall, 2007; Väisänen and Westerlund, 2007). Synvolcanic plutonic complexes are known to exist below volcanic piles at least in the Orijärvi (Colley and Westra, 1987; Väisänen *et al.*, 2002) and Enklinge areas (Ehlers *et al.*, 2004), but outside these two volcanic centres their areal extent is uncertain. Volcanism and plutonism of similar ages are also common in the Bergslagen area, south-central Sweden (Lundström *et al.*, 1998; Andersson *et al.*, 2006b; Hermansson *et al.*, 2008; Stephens *et al.*, 2009). As a consequence of convergence the southern Svecofennian arc complex was accreted to the central Svecofennian arc complex (Fig. 1B) at *c.* 1.87Ga. This is also the approximate age of most synorogenic plutonism (Väisänen *et al.*, 2002), which may therefore also be referred to as synaccretional plutonism. These rocks, the topic of this investigation, have the same field appearance as the synvolcanic intrusions, but differ in that the synorogenic intrusions crosscut the early deformation structures (Van Duin, 1992; Ehlers *et al.*, 1993; Nironen, 1999; Väisänen and Hölttä, 1999; Skyttä *et al.*, 2006; Hermansson *et al.*, 2007). The volcanic, synvolcanic and synorogenic magmatism have collectively been referred to as the early Svecofennian magmatism (*e.g.*, Gaál and Gorbatshev, 1987).

The continent-continent collision with Sarmatia, that took place at 1.84-1.79Ga in southern Finland, had severe effects in the southern Svecofennian arc complex. Rocks deformed and metamorphosed during arc-accretion were reworked and metamorphosed once again, but now at higher temperatures which caused crustal anatexis leading to the formation of the late-Svecofennian migmatites and

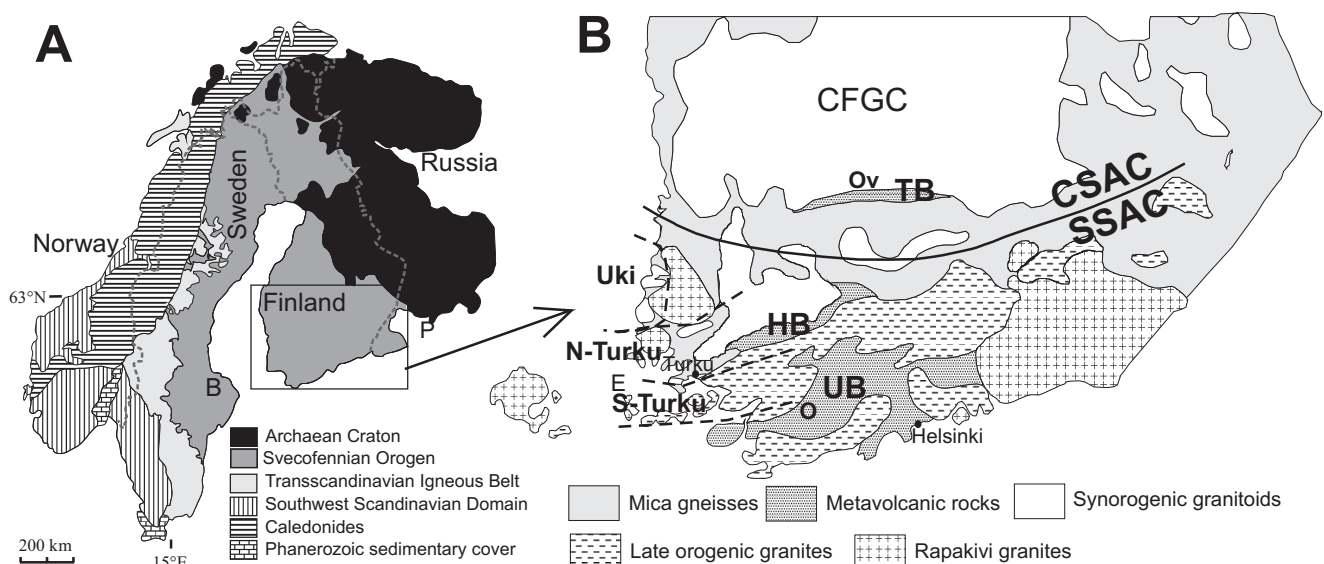


FIGURE 1 | A) Geological overview of the Fennoscandian Shield, modified after Högdahl and Sjöström (2001). B: Bergslagen, P: Puutsaari. B) Geological overview of southern Finland, modified after Korsman *et al.*, (1997). CFGC: Central Finland Granitoid Complex, CSAC: Central Svecofennian Arc Complex, E: Enklinge, HB: Häme Belt, O: Orijärvi, Ov: Orivesi, SSAC: Southern Svecofennian Arc Complex, UB: Uusimaa Belt. Study areas Uki, N-Turku and S-Turku are indicated.

granites (Huhma, 1986; Suominen, 1991; Ehlers *et al.*, 1993; Jurvanen *et al.*, 2005; Kurhila *et al.*, 2005, 2010; Skyttä and Mänttari, 2008). Upright folding refolded the previously gently dipping structures during dextral transpressional tectonics that subsequently led to the formation of steep shear zones (Ehlers *et al.*, 1993; Cagnard *et al.*, 2007; Väisänen and Skyttä, 2007; Torvela and Ehlers, 2010). The age of metamorphism is constrained by zircons from a leucosome intruding an upright F3 fold hinge which yielded an age of 1824 ± 5 Ma (Väisänen *et al.*, 2002), and the highest metamorphic conditions estimated for the migmatites are *c.* 6 kbar at 800°C (van Duin, 1992; Väisänen and Hölttä, 1999; Johannes *et al.*, 2003). Chardon *et al.* (2009) have therefore classified this part of the Svecofennian orogen as an ultra-hot orogen. A similar evolution also took place in central Sweden (*e.g.*, Högdahl *et al.*, 2008, 2009).

Because of the high-grade late Svecofennian overprint as well as inheritance in the zircon populations, the previously published U-Pb thermal ionization mass spectrometry (TIMS) zircon ages from the early Svecofennian granitoids have sometimes turned out to be mixed ages. It is only recently that a difference in age, structural character, and composition between the synvolcanic and synorogenic plutonic rocks have been identified. The distinction has been made possible by the recent advances in single zircon ion microprobe age determinations that have revealed the presence of inherited and metamorphic zircon domains (Väisänen *et al.*, 2002; Ehlers *et al.*, 2004; Andersson *et al.*, 2006b).

SAMPLE AREAS

Fieldwork and sampling were performed along a roughly north-south, *c.* 120 km-long transect across the east-west trending orogen in SW Finland. Altogether, sixty-two samples were collected for geochemical analyses (Table I, Electronic appendix available at www.geologica-acta.com), and two samples for U-Pb zircon dating (Table II) and Sm-Nd isotopic analysis (Table 1). The study area is divided into three main subareas (Fig. 1B).

The Uusikaupunki area (Uki)

This area was extensively studied by Hietanen (1943), who was the first to describe the trondhjemites and diorites/gabbros of the area. Arth *et al.* (1978) provided geochemical, Rb-Sr and oxygen isotopic analyses, and modelled the petrogenesis of the magmatic suite. Patchett and Kouvo (1986) performed U-Pb zircon age determinations and Sm-Nd isotope analyses on the same rock types. Their conventional TIMS dating on the trondhjemite samples yielded a range of ages between *c.* 1.89 and 1.96 Ga. Their preferred interpretation was that the trondhjemites had crystallized prior to 1.90 Ga, making them the oldest plutonic rocks in southern Finland. Their two diorite samples yielded TIMS ages of 1872 ± 11 Ma and 1874 ± 2 Ma. Selonen and Ehlers (1998) studied the structural setting of the trondhjemites and concluded that these were intruded as subhorizontal sheets, contained D2 structures and were refolded by F3 into steeper dips. In the descriptions cited above, the diorites are defined as hornblende-plagioclase-biotite rocks, tonalites as plagioclase-quartz-biotite±hornblende rocks and trondhjemites also as plagioclase-quartz-biotite rocks. In some varieties there are bigger quartz megacrysts, called drop-quartz trondhjemites by Hietanen (1943). Suominen *et al.* (2006), however, showed that the distinction between the trondhjemites and the tonalites was mainly based on estimates of colour and biotite content, where trondhjemites are lighter coloured. Modally, however, only small parts of the rocks are trondhjemites *sensu stricto*, since most of them contain too much biotite and occasionally even K-feldspar and pyroxene, which classifies them as tonalites and granodiorites. For consistency, however, we use the same rock names as Arth *et al.* (1978), Patchett and Kouvo (1986) and Suominen *et al.* (1994) because our sampling was guided by theirs, and because of geochemical differences between trondhjemites and tonalites as subdivided by them (Arth *et al.*, 1978 and this study; see also Fig. 6). No mafic enclaves were encountered in the trondhjemites in this study, but mafic inclusions are described in Suominen *et al.* (2006).

TABLE 1 | Sm-Nd isotope data from the Uusikaupunki area, southwestern Finland

Sample	Rock type	Locality	Sm (ppm) ¹	Nd (ppm) ¹	¹⁴⁷ Sm/ ¹⁴⁴ Nd ¹	¹⁴³ Nd/ ¹⁴⁴ Nd ± 2σ _m ² (measured)	ε _{Nd} ³ (present)	ε _{Nd} ³ (initial)	T _{CHUR} ⁴ (Ga)	T _{DM} ⁵ (Ga)
12-MJV-06	Trondhjemite	Uusikaupunki	1.30	6.62	0.1184	0.511812 ± 13	- 16.1	+ 2.6 (1867)	1.61	1.97
28-MJV-05	Diorite	Uusikaupunki	9.38	52.1	0.1088	0.511667 ± 8	- 18.9	+ 2.2 (1872)	1.68	2.00

¹Sm and Nd contents and ¹⁴⁷Sm/¹⁴⁴Nd ratio from isotope dilution analysis with combined ¹⁴⁷Sm-¹⁵⁰Nd tracer. Estimated analytical uncertainty of ¹⁴⁷Sm/¹⁴⁴Nd ratio is ±0.5 %

²¹⁴³Nd/¹⁴⁴Nd ratios calculated from ID run, corrected for Sm interference and normalized to ¹⁴⁶Nd/¹⁴⁴Nd = 0.7219. Two runs of the La Jolla Nd-standard during the measurement periods gave a ¹⁴³Nd/¹⁴⁴Nd ratio of 0.511857 ± 15 (2σ_m) and 0.511847 ± 6 (2σ_m), respectively. Error given as 2 standard deviations of the mean from the mass spectrometer run in the last digits.

³Present-day and initial ε_{Nd} values (at the given age), according to Jacobsen and Wasserburg (1984): present-day chondritic ¹⁴⁷Sm/¹⁴⁴Nd ratio 0.1967, present-day chondritic

¹⁴³Nd/¹⁴⁴Nd ratio 0.512638

⁴Model age calculated relative to the chondritic uniform reservoir (CHUR) of Jacobsen and Wasserburg (1984)

⁵Model age calculated relative to the depleted mantle curve (DM) of DePaolo (1981)

As the compositions of the rocks in this area show strong resemblance to rocks today described as TTGs (Arth *et al.*, 1978), this is a key area in the present study. Twenty-seven samples were selected from the Uki area for geochemical analysis. Because the age of the trondhjemites is enigmatic (*c.f.*, Patchett and Kouvo, 1986), one trondhjemite sample (type drop-quartz trondhjemite) was subjected to ion microprobe dating as well as one dioritic sample.

The north Turku area (N-Turku)

Located south of Uki and north of the town of Turku, this area contains relatively well-dated *c.* 1.87Ga intrusions that cut the earlier structures and are interpreted as synorogenic. Rock types are tonalites, trondhjemites and quartz diorites with some granodiorites. All the rocks were recrystallised in granulite facies (van Duin, 1992; Nironen, 1999; Väisänen *et al.*, 2002). Mafic enclaves are common in the felsic rocks (Fig. 2). Geochemical analyses in van Duin (1992) include high Sr and low Y rocks, indicating TTG-like signatures. Part of the rock suite is pyroxene-bearing, and was interpreted as a separate younger magmatic phase by Hietanen (1947) and van Duin (1992). The latter author interpreted a TIMS age of *c.* 1.84Ga as the time of magmatism. However, later investigations regard pyroxene and part of the zircons to be metamorphic and related to later post-magmatic processes and the intrusion age of these rocks is now regarded to be close to 1.87Ga (Väisänen *et al.*, 2002; Helenius *et al.*, 2004). Here, we include the pyroxene-bearing granitoids in the synorogenic group. Altogether, twenty-one samples were analysed for geochemistry.

The south Turku area (S-Turku)

From this area, located south of the town of Turku, no previous age or geochemical data are available. The field relationships, such as the intrusions cross-cutting early structural features indicate that these intrusions belong to the synorogenic group. Rock types are tonalites, quartz diorites and granodiorites; mafic enclaves are common in these rocks. Fourteen samples were analysed for geochemistry.

ANALYTICAL METHODS

U-Pb secondary ion mass spectrometer (SIMS) analyses

Zircons were imaged by back-scattered electrons (BSE) with a Cambridge Instruments Stereoscan 360 electron microscope at Åbo Akademi University, Turku, Finland. Measurement of Pb/Pb isotope ratios and U, Th, and Pb concentrations were performed on the Cameca IMS 1270

ion microprobe of the NORDSIM facility at the Swedish Museum of Natural History following methods described by Whitehouse *et al.* (1999) and Whitehouse and Kamber (2005). A flat-bottomed spot with a diameter less than 20µm was achieved using a 150µm aperture inserted into the defocused primary beam. The resulting primary ion current (O_2^-) was typically *c.* 4nA. Measurements were taken over 12 cycles through the respective mass stations measured in peak skipping mode. U/Pb ratio calibration was based on analyses of the standard zircon 91500 (Wiedenbeck *et al.*, 1995) and used a best-fit power law relationship of U_2O/U versus U/Pb. The common Pb correction is assumed to represent present day surface contamination and is effectively corrected using the present-day terrestrial average Pb-isotopic composition of Stacey and Kramers (1975) *i.e.*, $^{207}Pb/^{206}Pb=0.83$, which has been shown to be appropriate for this laboratory (Kirkland *et al.*, 2008). The data were calculated and plotted using the Isoplot program (Ludwig, 2003). The analyses were performed during the same sessions as those published in Väisänen and Kirkland (2008), where a more detailed method description is found.

Sm-Nd analyses

Whole-rock powders of the investigated rocks have been analysed for their Sm and Nd contents and Nd isotope compositions at the Laboratory for Isotope Geology of the Swedish Museum of Natural History. For the analyses, 150–200mg of rock powder was mixed with an appropriate amount of mixed ^{147}Sm - ^{150}Nd tracer, and dissolved in HF and HNO_3 (concentrated 10:1 mixture) in teflon capsules in an oven at 205°C for a few days. After evaporation, the samples were redissolved, first in 5ml 6M HCl at 205°C overnight, and then in 1ml 2.5M HCl at 60°C overnight. After centrifuging to obtain a clear solution, REE as a group was separated from the solution using standard cation exchange procedures with HCl and HNO_3 as media. The



FIGURE 2 | Mafic enclaves in tonalite, N-Turku area. Width of the photograph is 50cm.

REE fractions were evaporated and redissolved in 0.05M HNO₃, and Sm and Nd separated from each other with HCl using the Ln-spec method (Pin and Zalduegui, 1997).

Samarium was analyzed in static mode, and neodymium in multi-dynamic mode on a Finnigan MAT261 mass spectrometer, with corrections for isobaric interferences and fractionation as reported in the footnotes to Table 1. Results of repeated runs of the La Jolla Nd-standard are also reported there. Sm and Nd concentrations, and Nd isotope compositions, were computed from the spiked analyses. T-CHUR Nd model ages have been calculated according to Jacobsen and Wasserburg (1984) and T-DM model ages according to the Depleted Mantle curve of De Paolo (1981).

Major and trace element analyses

Fifty samples were analysed at Acme Analytical Laboratories Ltd. (Acme) in Vancouver, Canada. The samples were pulverised in a mild steel swingmill and after the LiBO₂ fusion and HNO₃ dilution, the major elements, Cr, and Sc were analysed by inductively coupled plasma-emission spectrometry (ICP-ES). The other trace elements were analysed by inductively coupled plasma-mass spectrometry (ICP-MS). The analytical precision is 1-5% for the major oxides and ±10 % for the other elements.

Nine samples were analysed at Activation Laboratories Ltd. (Actlabs), Ancaster, Canada. The samples were pulverised in a mild steel swingmill. After the lithium metaborate/tetraborate fusion, the major elements were analysed by ICP-ES and the trace elements by ICP-MS. The relative standard deviations from replicate analyses are ≤3% for major elements and ≤5% for trace elements.

Three samples were analysed at the Geological Survey of Finland. The samples were pulverised in a carbon steel grinding vessel. The major elements, Ba, Cr, Cu, Ni, Pb, Rb, Sr, V, Zn, and Zr were analysed by X-ray fluorescence (XRF) on pressed powder pellets. The other elements were analysed by inductively coupled plasma-mass spectrometry (ICP-MS) after hydrofluoric-perchloric acid dissolution. The geochemical analyses were plotted using the GCDkit software (Janoušek *et al.*, 2006).

RESULTS

U-Pb zircon and Sm-Nd whole rock analyses

Uusikaupunki trondhemite (12MJV06)

The zircon crystals from the trondhemite sample are very heterogeneous in shape with both elongate prismatic (100-200µm in length) and stubby or rounded crystals

(c. 40-15µm). From the backscattered electron (BSE) images it is evident that most zircons have cracks and metamict areas. Internal (growth) zoning is common. Most zircons also have a homogeneous BSE-bright outer rim (without zoning) that occasionally clearly crosscuts the inner zoning. In some cases, homogeneous patches also overprint the inner domains. The rims are often affected by metamictization (Fig. 3A-D).

Twenty-five spots on eighteen different zircons were analysed (Appendix, Table II). Most spots were obtained from the prismatic zircons and the inner zoned regions. Few spots were aimed at the outer rims. Because of cracks, metamict domains and narrowness of the outer rims, it was difficult to find large enough intact areas to place the spots. This has caused many analyses to hit cracks, metamict domains or epoxy, leading to discordancy. Some analyses might be mixtures of core and rim domains. Some core domains of the zircons contained inherited cores of Archaean age (2667Ma, slightly discordant) as well as early Palaeoproterozoic ²⁰⁷Pb/²⁰⁶Pb ages (concordant 2165 and 1965Ma, as well as discordant 2073Ma ²⁰⁷Pb/²⁰⁶Pb ages; Fig. 4A). Twelve of the analyses from the prismatic crystals and the zoned inner domains yielded a weighted average ²⁰⁷Pb/²⁰⁶Pb age of 1867.5±3.1Ma (mean square weighted deviation, MSWD=1.12) and a concordia age of 1866.5±3.8Ma, MSWD=9.4; Fig. 4B). Therefore, we consider that 1867±4Ma is the best estimate for the crystallisation age of the trondhemite magma. Three analyses obtained from the homogeneous BSE-bright rims and patches yielded an upper intercept age of 1842±5Ma (MSWD=0.041; Fig. 4C). This age is based on only three analyses, two of which are discordant. However, one of the three analyses is concordant with a ²⁰⁷Pb/²⁰⁶Pb 2σ age of 1843±8Ma (n2394-18c in Table 1). We interpret this age to reflect metamorphic zircon growth at c. 1.85-1.84Ga.

Whole rock Sm-Nd isotopic analysis of the same sample yielded an initial (at 1867Ma) ε_{Nd} value of +2.6 (Table 1), indicating a mildly depleted mantle source or a juvenile crustal source for the magma.

Uusikaupunki diorite (28MJV05)

The zircon crystals from the diorite sample are of variable shape and size, but most are euhedral to subhedral in shape and 100-300µm in length. Broken crystals of this size indicate that even bigger crystals existed. The most striking feature is that all the zircons are internally quite homogeneous and (growth) zoning, or separate core domains, are not obvious in the BSE images. Some crystals show a very narrow metamict outer rim. Cracks are common (Fig. 3E-F).

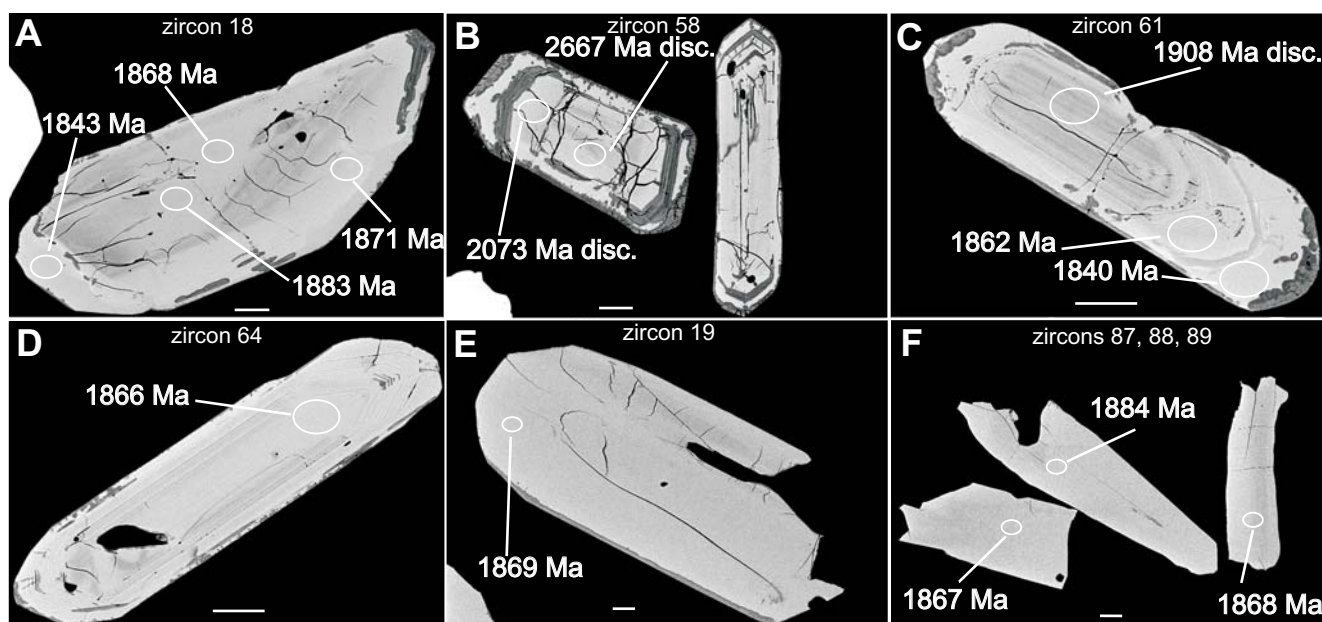


FIGURE 3 | Back-scattered electron (BSE) images of selected zircons. 3A-3D are from the Uusikaupunki trondhjemite and 3E-3F are from the Uusikaupunki diorite. The trondhjemite zircons show narrow homogeneous rims, partly metamict, on zoned inner domains. Rims are thickest on the tips of the zircons and ages 1843Ma in A and 1840Ma in C) come from such rims. Core domain in zircon 58 in B was slightly discordant (disc.) but evidently show Archaean c. 2.7Ga age; c. 2.1Ga rim domain is discordant. The prismatic zircon on the right side in B was not analysed. One of the analyses in the inner domain of the zircon 61 in C was discordant and was not used in the age calculation. The diorite zircons in 3E and 3F are homogeneous with only a narrow metamict rim in E and some cracks. White scale bar on the lower part of each figure is 20 μ m long. Ages refer to $^{207}\text{Pb}/^{206}\text{Pb}$ ages shown in Appendix, Table II.

Forty-one spots in forty-one different zircon crystals were analysed (Appendix, Table II). All error ellipses plot concordant or near concordant and form a cluster at c. 1.87Ga. Excluding three discordant analyses, a concordia age of $1872 \pm 3\text{Ma}$ (MSWD=1.5) is obtained (Fig. 4D). We interpret this to date the crystallisation of the diorite magma.

Whole rock Sm-Nd isotopic analysis of the same sample yielded an initial (at 1872Ma) ϵ_{Nd} value of +2.2 (Table 2), again indicating a mildly depleted mantle source or a juvenile crustal source for the magma.

Geochemistry

Major elements

The silica content of all samples ranges between c. 56 and 72 wt% (Appendix, Table I; Fig. 5). The Uki samples are distributed in two principal compositional groups: i) diorites with $\text{SiO}_2 \leq 61\text{wt}\%$, and ii) and a suite of tonalites/granodiorites/trondhjemites ranging in composition from 63 to 72% SiO_2 . Using the normative An-Ab-Or diagram of Barker (1979), all the samples previously referred to as trondhjemites plot in the proper field while some of the other samples show slight deviations from their previous names (Fig. 6). The N-Turku and the S-

Turku samples have intermediate SiO_2 contents. All samples have silica contents above 56 wt%, consistent with definitions of adakite (Martin *et al.*, 2005), and except the diorites all samples have SiO_2 contents $>60\text{wt}\%$ as defined for high-silica adakite. Compositions $>64\text{wt}\%$ SiO_2 have been suggested to apply for TTG rocks (Martin *et al.*, 2005), and most of the tonalite-trondhjemite samples fulfil this criterion (Fig. 5). With a few exceptions, the samples show variable but high contents of Al_2O_3 and Na_2O , typical of adakites (Fig. 7). Apart from the Uki diorites, MgO contents are below the 4wt% characteristic for HSA (*c.f.*, Martin *et al.*, 2005). TiO_2 contents are also low, as expected for adakites (Appendix, Table I). $\text{K}_2\text{O}/\text{Na}_2\text{O}$ ratios of the present samples overlap the compositional fields of high-silica adakites, and those of the tonalite-trondhjemites are typical for TTGs (*c.f.*, Condie, 2005; Moyen, 2009), except for two outlier samples. The magnesium numbers (Mg#) are systematically high, ≥ 55 , only in the Uki diorite samples. The Uki tonalites have moderate values (38-48) and the trondhjemites show low values (32-42). The N-Turku and the S-Turku samples has the largest Mg# range (30-55), generally below the average adakitic value of ~ 51 , except for some of the N-Turku samples (Fig. 7F), in which the tonalite-trondhjemites overlap the Mg# reported for HSA (Martin *et al.*, 2005). Most of the tonalite and trondhjemite samples are calc-alkaline, whereas most of the diorite samples from Uki plot in the high-K calc-alkaline field (Fig. 7D).

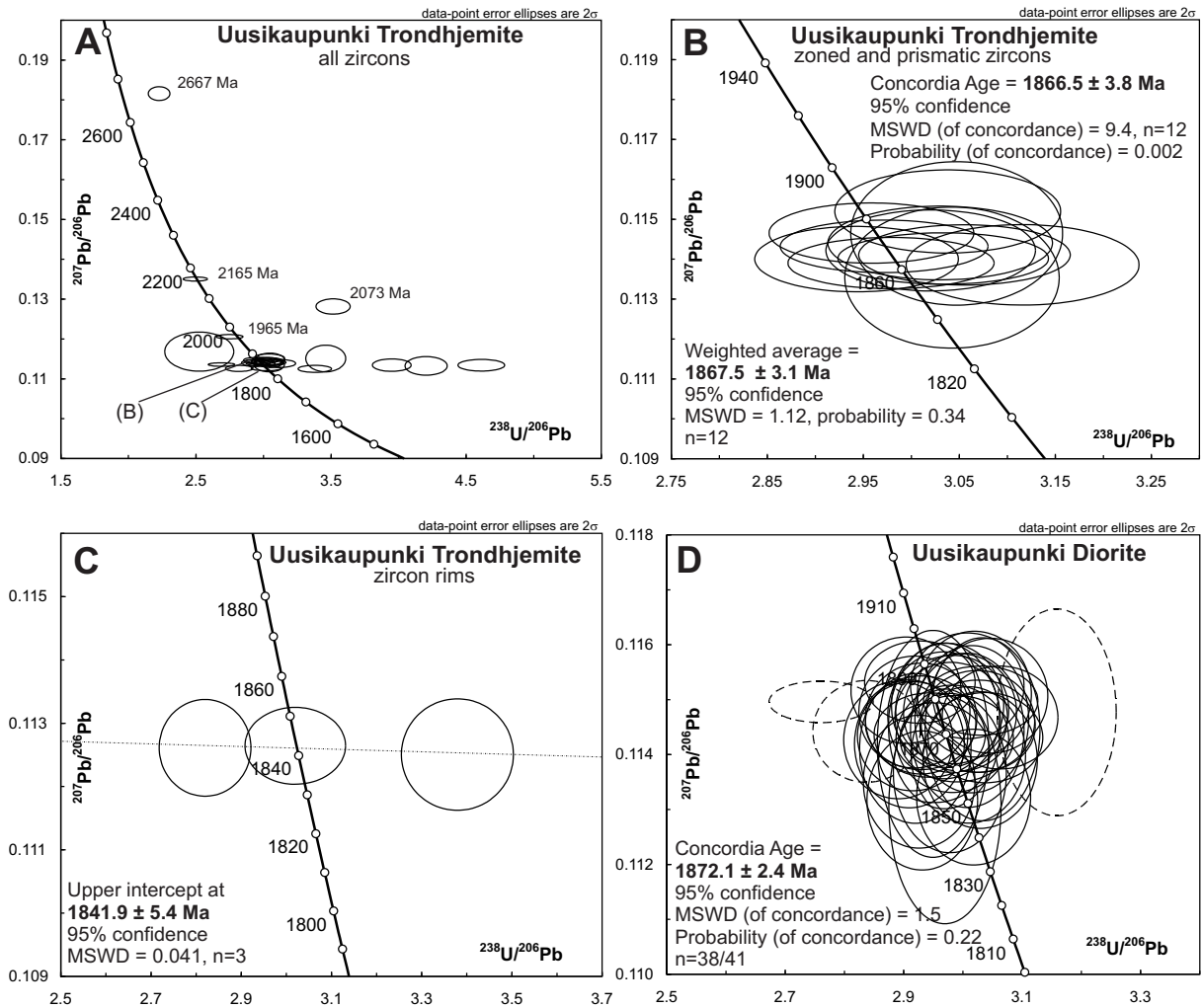


FIGURE 4 | Tera-Wasserburg concordia diagrams for the ion microprobe analyses on zircons from the samples A-C) Uusikaupunki trondhjemite and D) Uusikaupunki diorite. A) shows all analyses performed on the trondhjemite sample. The four oldest $^{207}\text{Pb}/^{206}\text{Pb}$ ages are shown by the side of the error ellipses. The majority of analyses form a cluster between 1900 and 1800 Ma. The cluster is zoomed in B and C. In the diorite sample (D) the discordant analyses excluded from the age calculation are shown with dashed lines.

Trace elements

The most commonly used trace elements that effectively discriminate adakites and TTGs from the mantle wedge-derived volcanic arc magmatic rocks are Sr, Y, La and Yb and their ratios because of their sensitivity to pressure during magmatic processes (*e.g.*, Martin *et al.*, 2005). Sr contents are high (>400ppm, Fig. 8A) in most samples, apart from the S-Turku samples where about half of the samples have Sr<400ppm. Y and Yb contents on the other hand are low (generally <18 and 1.9ppm, respectively; Fig.8B, D), contributing to high Sr/Y and La/Yb ratios (Fig. 8E-F). It is noteworthy that some of the N-Turku and S-Turku samples that plot below the cut-off value of 40 in the Sr/Y diagram, plot above the cut-off value of 20 in the La/Yb diagram, however. These ratios form the basis for the most commonly used Sr/Y vs Y and La/Yb vs Yb

discrimination diagrams to differentiate adakites and TTGs from other volcanic arc magmas (Fig. 9). The present samples in general plot within the adakite/TTG fields with a few exceptions from the N-Turku and S-Turku areas. The Uki diorites form a separate group that plots transitional into the volcanic arc field (Fig. 9).

In accordance with the high Mg#, the Uki diorites as well as some of the N-Turku samples have high contents of Ni and Cr, fulfilling the adakitic criteria. The Uki trondhjemites and tonalites and most of the S-Turku samples have low contents of Ni and Cr (Fig. 8G-H), lower than in adakites in general.

In the chondrite normalized REE diagrams (Fig. 10) most trondhjemites show positive Eu anomalies, while the tonalites show no anomalies. Both have low heavy rare

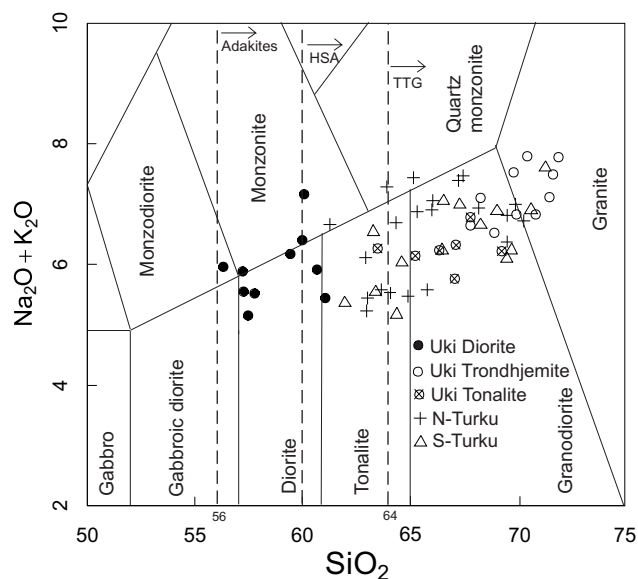


FIGURE 5 | Total alkali vs. SiO_2 (TAS, in wt%) diagram after Middlemost (1994) with added SiO_2 division lines for adakites, high-silica adakites (HSA) and tonalites-trondhjemites-granodiorites (TTG) after Martin *et al.* (2005).

earth element (HREE) and high, light rare earth elements (LREE) contents, and thus high, LREE/HREE ratios. The N-Turku and S-Turku samples show similar, but more variable characteristics, and have both positive and slightly negative Eu anomalies. The diorites have the highest HREE contents and lowest LREE/HREE ratios.

In the primitive mantle-normalized multi-element diagrams (Fig. 10), the diorites show negative or no Sr anomalies as well as negative Zr and Ti anomalies. HREE contents in diorites are higher than in all the other groups. The Uki trondhjemites show positive Sr and Zr anomalies, a very small negative or no Ti anomaly, and very low HREE contents. The tonalites show both positive and negative Sr and Zr anomalies and slightly negative Ti anomalies. HREE contents are low, but higher than in the trondhjemites. The samples from N-Turku resemble the tonalite samples in their slightly positive Sr and negative Ti anomalies. Samples from S-Turku show the most scatter and display positive, no and negative anomalies for Sr and Ti, and a weak positive or no Zr anomaly. All the samples show pronounced negative Nb anomalies (also Ta, not shown).

DISCUSSION

Age constraints

Recent findings have called into question whether the so-called early Svecofennian plutonism actually is a homogeneous suite of rocks, or rather should be subdivided into at least two different magma generations: an older preorogenic

(*i.e.*, synvolcanic) stage and a younger synorogenic one. The idea of two magma generations is supported by recent single zircon ion microprobe datings, (Väisänen *et al.*, 2002, Vaasjoki *et al.*, 2003; Ehlers *et al.*, 2004; Högdahl *et al.*, 2008). The synorogenic magmatism from southern Finland has ages between *c.* 1875Ma and 1860Ma, peaking at about 1.87Ga (Patchett and Kouvo, 1986; Suominen, 1991; van Duin, 1992; Nironen, 1999; Väisänen *et al.*, 2002; Skyttä *et al.*, 2006; Pajunen *et al.*, 2008), *i.e.*, *c.* 10-40 million years younger than the preorogenic plutons, which formed synvolcanic magma chambers, and are dated at 1896 ± 3 Ma in Orivesi (Talikka and Mänttari, 2005), 1898 ± 9 Ma in Orijärvi (Väisänen *et al.*, 2002) and 1884 ± 5 Ma in Enklinge (Ehlers *et al.*, 2004; Fig. 1B). Similar preorogenic ages have been obtained from volcanic and plutonic rocks in the Bergslagen area, south-central Sweden (*e.g.*, Andersson *et al.*, 2006b; Stephens *et al.*, 2009).

The Uki diorite yielded a well-defined age of 1872 ± 3 Ma, overlapping the previous age determinations within error on the same rock type (Patchett and Kouvo, 1986) and confirming that these were not mixed ages. This may be related to the homogeneous zircon morphology, with absence of older cores and younger rims in the diorite sample, which is in strong contrast to the zircons in the trondhjemite sample. Our preferred interpretation is that the mantle-derived diorite magma was not strongly contaminated by older crustal material during ascent. Alternatively, if any crustal contamination took place, xenocrystic zircons were totally consumed in the hot mafic magma.

The previously reported heterogeneous zircon TIMS ages of the Uki trondhjemites (older than 1.90Ga; Patchett and Kouvo, 1986) most probably resulted from mixtures of age populations in the zircon fractions as shown by the

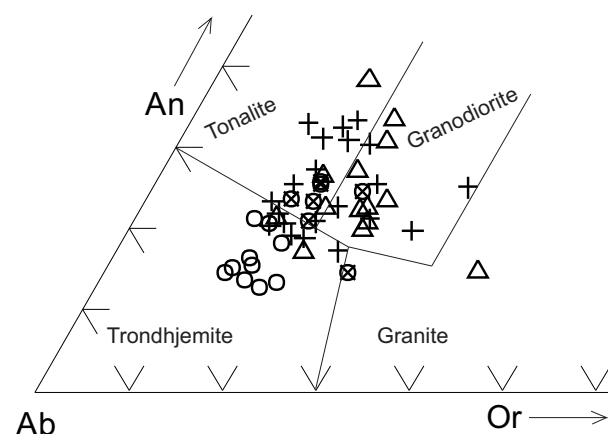


FIGURE 6 | Normative An-Ab-Or diagram (Barker, 1979) to discriminate trondhjemites from other granitoids. Norms calculated by SINCLAS (Verma *et al.*, 2002). The Uki diorites were omitted for clarity. Symbols as in Figure 5.

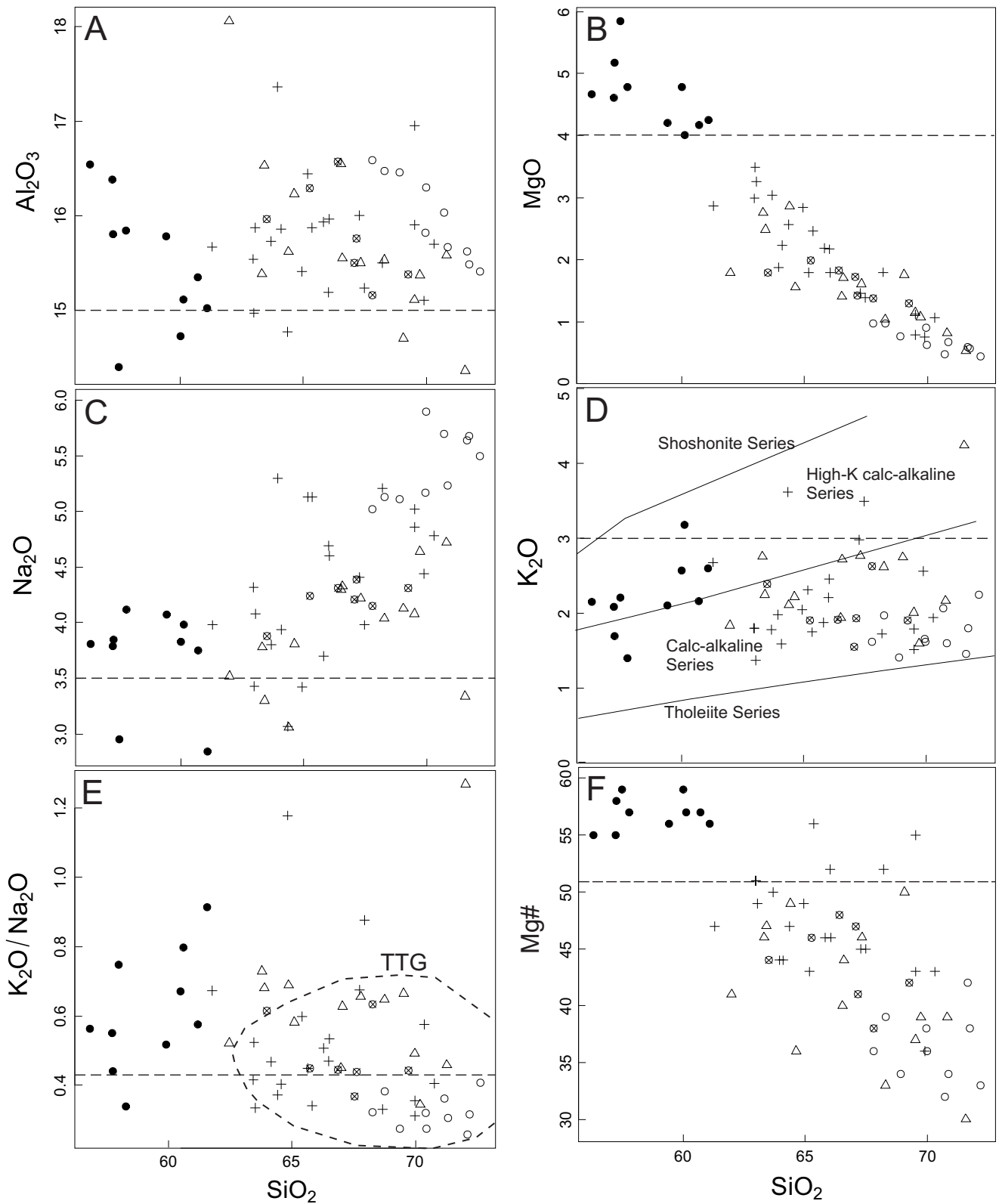


FIGURE 7 | Selected major elements, K₂O/Na₂O and Mg# vs. SiO₂ diagrams. Defining values (dashed lines) for high-silica adakites are: A) Al₂O₃ ≥ 15wt%, B) MgO ≤ 4wt%, C) Na₂O ≥ 3.5wt%, D) K₂O ≤ 3wt% according to Richards and Kerrich (2007), E) K₂O/Na₂O ~ 0.42, F) Mg# ~ 51. Fields in D are according to Peccerillo & Taylor (1976). Tonalites-trondhjemites-granodiorites field in E (dashed line) after Moyen (2009). Symbols as in Figure 5.

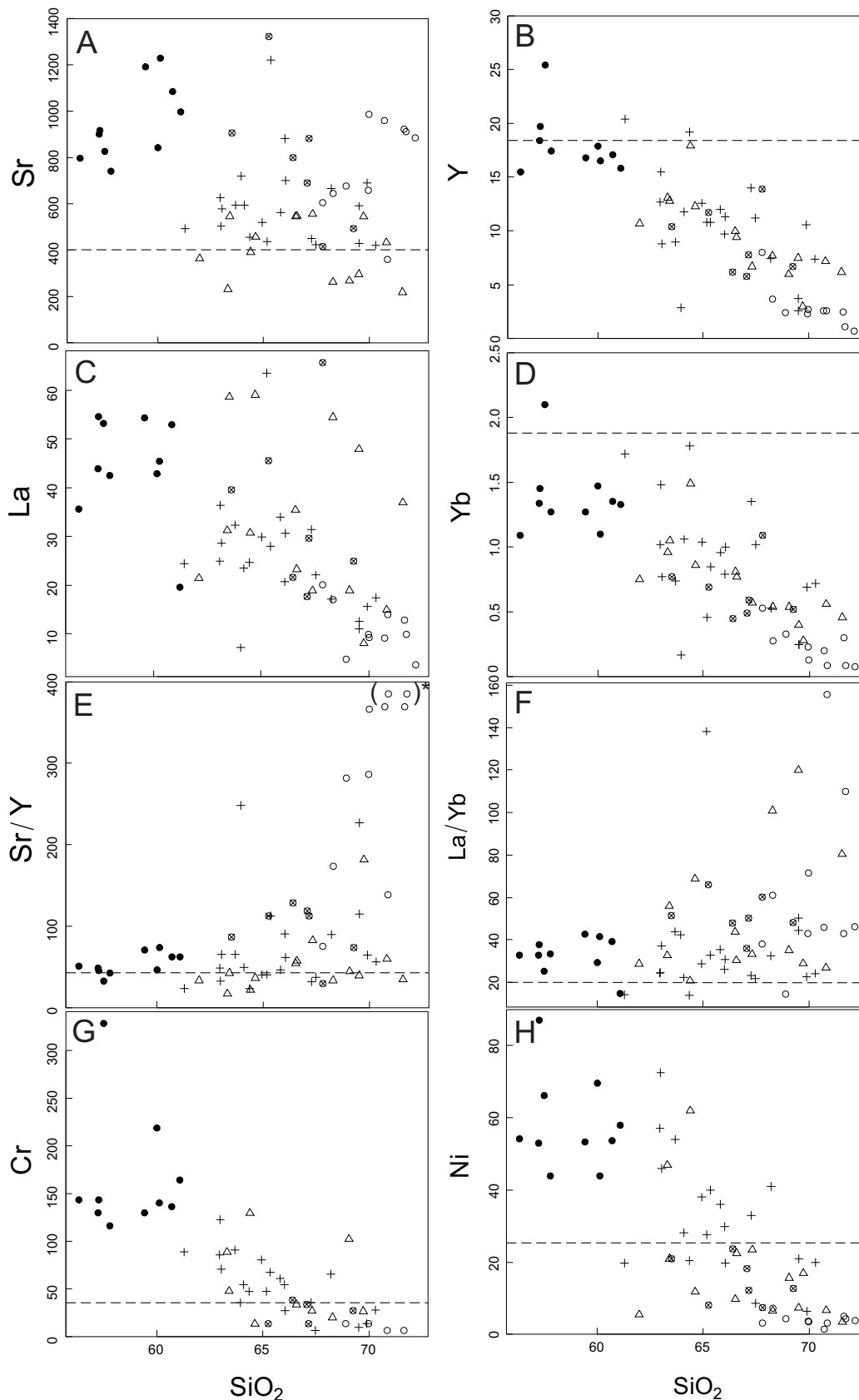


FIGURE 8 | Selected trace element and trace element (in ppm) ratios vs. SiO₂ (in wt%) diagrams. Defining values (dashed lines) for high-silica adakites are: A) Sr > 400, B) Y < 18, D) Yb < 1.9, E) Sr/Y > 40, F) La/Yb > 20, G) Cr ~ 24, H) Ni ~ 36. In E two trondhjemite samples have elevated values (829 and 1265), outside the diagram, indicated by (oo)*. Symbols as in Figure 5.

present results. A number of SIMS spots in crystal domains with igneous zoning yielded an intrusion age of 1867Ma for the trondhjemite magma, while inherited core domains gave late Archaean and early Palaeoproterozoic ages, and metamorphic rims an age of *c.* 1.84Ga. The crystallization age clearly puts the trondhjemites into the *c.* 1.87Ga synorogenic age group. The inherited Archaean and early Palaeoproterozoic ages can be interpreted in three ways, i) the 1867Ma trondhjemite magma was generated from crust comprising rocks of such ages or ii) it was generated from crust with sediment intercalations which contained older detrital zircons of such ages or iii) the ascending trondhjemite magma assimilated crustal material containing such detrital zircons.

However, the positive initial ϵ_{Nd} values between +1.7 and +2.6 (Patchett and Kouvo, 1986; this study) exclude a major Archaean influence on these rocks, and show that the trondhjemite magma was dominated by mantle or juvenile crustal components. Svecofennian metasediments are known to contain *c.* 30% Archaean and 70% Palaeoproterozoic detrital zircons having ages similar to those obtained here (*e.g.* Claesson *et al.*, 1993; Andersson *et al.*, 2006b; Bergman *et al.*, 2008; Lahtinen *et al.*, 2009). ϵ_{Nd} (1.87Ga) values of the Svecofennian metasediments are significantly lower than those of the trondhjemites, essentially in the range -1.5 to -7 (*e.g.*, Claesson, 1987; Huhma, 1987; Patchett *et al.*, 1987; Claesson and Lundqvist, 1995; Andersson *et al.*, 2002), which exclude the metasediments as the sole source. In contrast, the ϵ_{Nd} values of the trondhjemites fall in the upper part of the range for 1.91-1.86Ga felsic Svecofennian metaigneous rocks (*c.f. e.g.*, compilations in Andersson *et al.*, 2002; Rutanen *et al.*, 2011), with T-DM ages around 2.0Ga. The Nd isotopes thus allow a derivation of the trondhjemites from such juvenile crustal lithologies. The presence of juvenile 2.1-1.91Ga Svecofennian crust has been inferred from several lines of evidence (*e.g.*, Lahtinen and Huhma, 1997; Andersen *et al.*, 2009). In addition, at least some of the inherited zircons could come from sedimentary intercalations, containing Archaean components.

The younger 1842±5Ma rims on the *c.* 1.87Ga trondhjemite zircons are interpreted as metamorphic. This is one of the oldest ages reported for late-Svecofennian metamorphism in southern Svecofennian arc complex so far. Torvela *et al.* (2008) also reported 1850±12Ma metamorphic rims on older magmatic zircons, but that age was based only on one single spot. Furthermore, their sampling site is to the south of the South Finland shear zone, which is interpreted as a terrane boundary and the southern border of the high grade southern Svecofennian arc complex (Torvela and Ehlers, 2010). Previously, the peak metamorphism and the age of the crustally derived granites were constrained between *c.* 1.83 and 1.81Ga (Korsman

et al., 1984; Huhma, 1986; Suominen, 1991; Väisänen *et al.*, 2002; Jurvanen *et al.*, 2005; Mouri *et al.*, 2005; Skyttä and Mänttari, 2008; Väisänen and Kirkland, 2008). The 1842±5Ma age indicates that metamorphic temperatures were high enough to crystallize new zircon at that time, supported also by the generation of crustally derived anatectic granites of similar ages (1.85-1.84Ga; Romer and Öhlander, 1995; Kurhila *et al.*, 2005, 2010; Hermansson *et al.*, 2007; Skyttä and Mänttari, 2008; Nironen and Kurhila, 2008).

Source region of magmatism

Uki

In spite of overlapping Nd isotopic data, several lines of evidence in the geochemical data suggest that the mafic and felsic magmatism in the Uki area have different sources. The first argument comes from the major element data where the gap in silica contents (Fig. 5) is inconsistent with fractionation of mafic magma leading to tonalites and trondhjemites (Arth *et al.*, 1978), as such a process would be expected to generate more intermediate compositions. Secondly, the geochemical trends are also inconsistent with fractionation. For example, the K₂O contents are the same or higher in the diorites compared to the tonalites and trondhjemites, which would require the removal of K-feldspar or biotite during fractionation, which finds no support petrographically (Fig. 7D). Furthermore, the combination of trends for Al₂O₃, Na₂O, and Sr are contradictory with respect to plagioclase fractionation, while the strongly decreasing trends for Y and HREE would require the removal of garnet or zircon which is also not corroborated by petrography.

The relatively high MgO, Mg#, Ni and Cr contents (Figs. 7, 8) in the diorite samples suggest that they are derived from a mantle source, or that they are slab melts. However, the idea of slab melts contaminated by interaction with mantle wedge peridotites, leading to low-silica adakites (*c.f.* Martin *et al.*, 2005), is not supported by other data for the diorites. The Y and Yb contents of the diorites are among the highest of all the data in the present set, and their moderate Sr/Y and La/Yb ratios mainly depend on their high La and Sr contents (Fig. 8A, D). This makes them plot on the boundary between the adakites/TTGs and volcanic arc magmas (Fig. 9), and below the typical values for low-silica adakites. A garnet-bearing source is therefore not supported, and the diorites are ambiguous adakites. Therefore, a source in the uppermost, spinel lherzolitic portion of the mantle is more likely. The relatively high K₂O and LREE contents of the diorites suggest that the mantle portion was enriched during previous subduction, supported by the negative anomalies for Nb, Zr and Ti (Fig. 10), typical for subduction-related magmatism (*e.g.*, Pearce, 1996). However, the enrichment is not at all as pronounced as that in the post-

collisional, high-K and shoshonitic *c.* 1.8Ga magmatism, which later intruded into the same region (Andersson *et al.*, 2006a; Rutanen *et al.*, 2011 and references therein).

The tonalites and trondhjemites in the Uki area have most of the characteristics defined for adakite- and TTG-like magmas. They plot in the appropriate fields in the Sr/Y vs Y and La/Yb vs Yb diagrams (Fig. 9). Furthermore, in many cases they have positive Eu and Sr anomalies (Fig. 10), suggesting that no plagioclase remained in the source and that some accumulation of plagioclase instead occurred. The typically low HREE contents lead to high La/Yb ratios (Fig. 8F), indicating that garnet remained in their source (*c.f.*, the low-HREE TTG of Halla *et al.*, 2009). However, the MgO, Mg#, Ni and Cr contents are consistently lower than is typical for slab-derived adakites. We interpret this to mean that these melts never interacted with mantle wedge peridotites, in accordance with Smithies (2000) and Condie (2005). In addition, the tonalites show rather high K₂O/Na₂O ratios. The trondhjemites have exceptionally high Na₂O contents, making their K₂O/Na₂O ratios very low. Most samples plot in the TTG field as defined by Moyen (2009; Fig. 7E). All combined, these geochemical characteristics are typical for crustally derived high-silica adakite/TTG-like rocks, inferred to be derived from the mafic lower crust (*c.f.*, Muir *et al.*, 1995; Smithies, 2000; Huang *et al.*, 2009; Moyen, 2009). The tonalites consistently show intermediate compositional characteristics, between those of the trondhjemites and diorites, but plot closer to the trondhjemites. This, and the common occurrence of mafic magmatic enclaves, strongly suggest that they carry a component of mafic admixture from the diorites. The rather high contents of the large ion lithophile element (LILE), as well as the negative Nb and Ti anomalies visible in the multi-element diagrams (Fig. 10) point towards a subduction component. This is natural as the Svecofennian crust was formed from juvenile sources in volcanic arc/continental margin settings 200–10 million years earlier (Huhma, 1986; Patchett and Kouvo, 1986; Lahtinen and Huhma, 1997; Ehlers *et al.*, 2004; Kähkönen, 2005; Andersson *et al.*, 2006b; Andersen *et al.*, 2009). Remelting of this source would be expected to produce arc-type signatures and readily account for the positive ϵ_{Nd} values between +1.7 and +2.6. Higher values would be expected if the source was completely juvenile and lower values if the source was older.

N-Turku

The composition of samples from the N-Turku area is highly variable. In terms of MgO, Mg#, Ni and Cr many of the N-Turku samples plot in between the mantle-derived mafic Uusikaupunki diorites and the more

felsic crustal-derived granitoids (Figs. 7, 8). In most diagrams presented here many of the samples seem to be true adakites. In the Sr/Y vs Y and (La/Yb)_N vs (Yb)_N discrimination diagrams (Fig. 9) a few of the samples plot outside the proper adakite/TTG field, in the transitional field or in the volcanic arc field, together with the Uusikaupunki diorites. In contrast, some samples have high Sr/Y and La/Yb ratios, resembling the Uki granitoids. The REE and multi-element diagrams show the same; a few of the analyses have positive Eu and Sr anomalies and very low HREE contents, but most are similar to the tonalites from the Uki area (Fig. 10). Intrusions in the N-Turku area thus seem to comprise rocks ranging from mantle to crustal in signature. However, only one sample has such a low SiO₂ content as

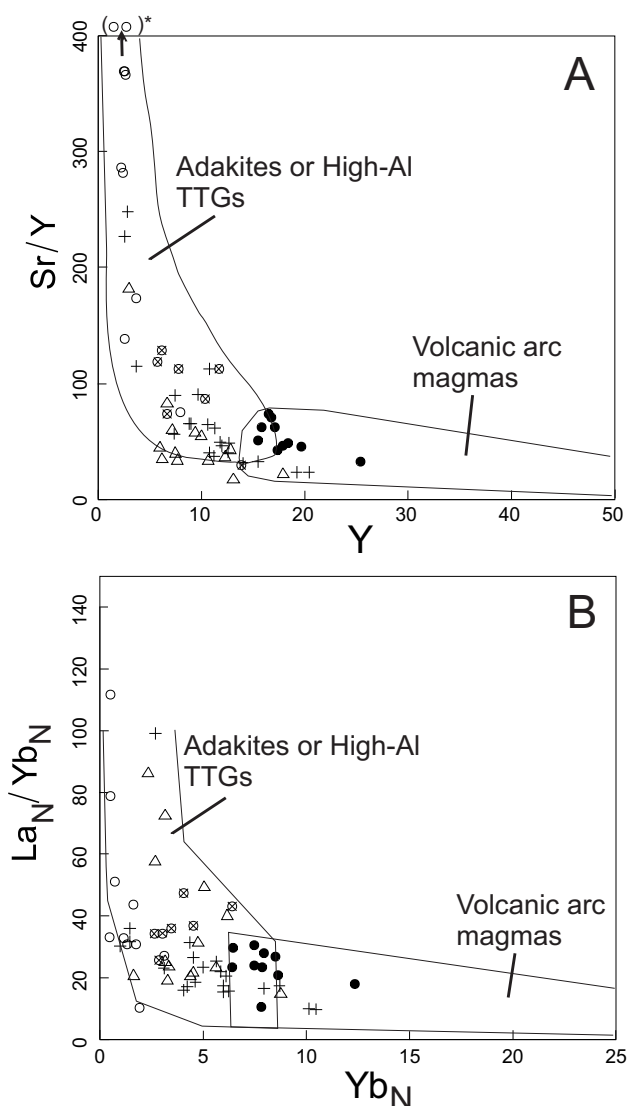


FIGURE 9 | A) Sr/Y vs. Y (after Defant and Drummond, 1990) and B) (La/Yb)_N vs. (Yb)_N (after Martin, 1999). In A two trondhjemite samples have elevated values (829 and 1265) outside the diagram, indicated by (oo)*. Symbols as in Figure 5. Units in ppm.

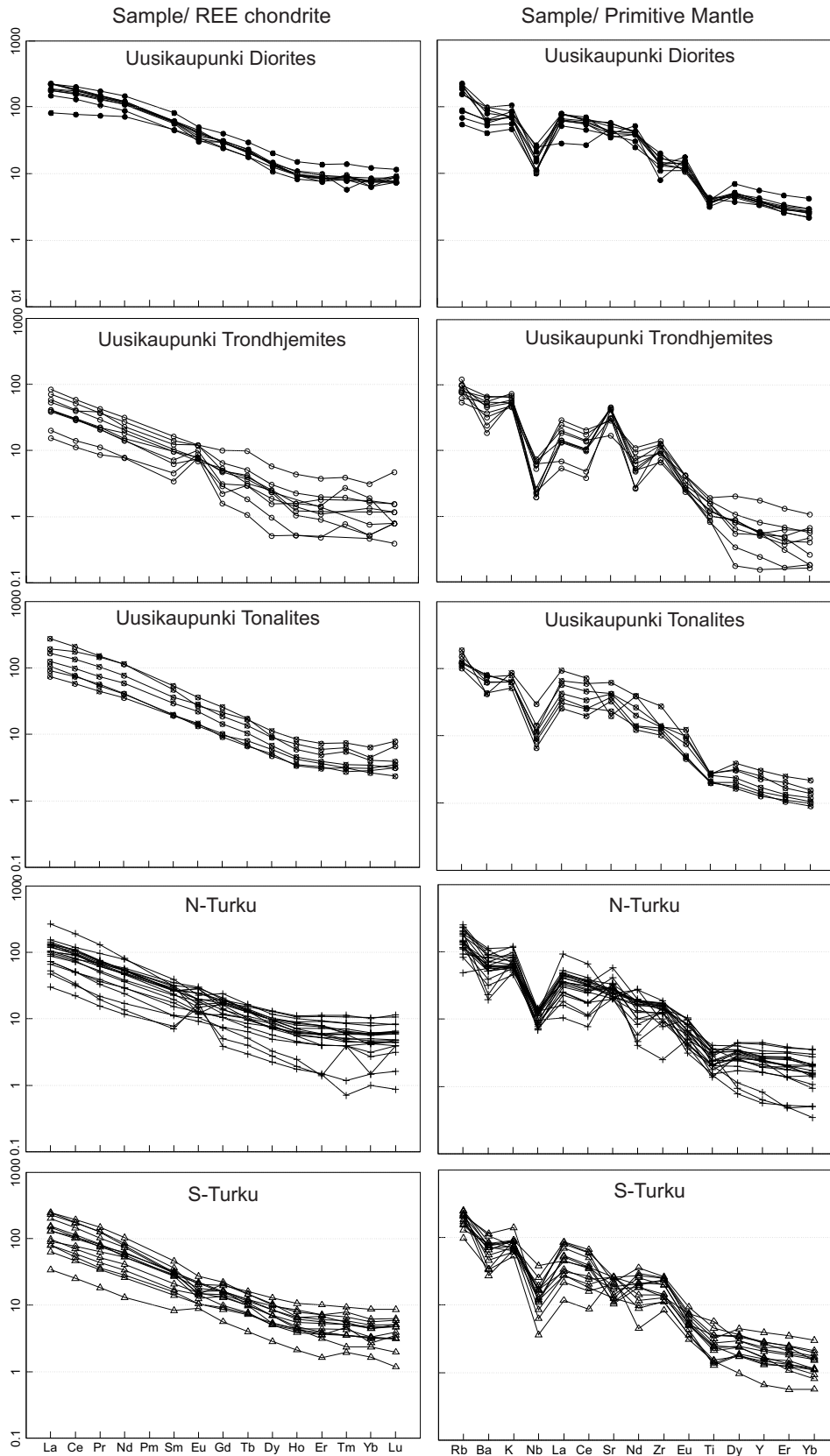


FIGURE 10 | Chondrite normalized REE diagrams (left column) and primitive mantle normalized multi-element diagrams (right column). Normalization values after Sun and McDonough (1989). Symbols as in Figure 5.

the Uki diorites, and the MgO contents are systematically lower. We suggest that the high Mg, Ni and Cr rocks are hybrids between mantle-derived and crustal melts. The N-Turku felsic granitoids contain abundant mafic enclaves which might represent the mafic member, the mafic member (Fig. 2). A published ion microprobe zircon dating of a hornblende tonalite (sample 110-MAV-02 in Appendix, Table I) yielded a crystallisation age of *c.* 1.87Ga, but the zircons contained inherited cores of Archaean and older Palaeoproterozoic age (Väisänen *et al.*, 2002), strikingly similar to the zircons in the trondhjemite sample in this study, thus verifying a crustally derived source component. The process here resembles the one referred to as MASH (melting, assimilation, storage, homogenization) by Hildreth and Moorbath (1988).

S-Turku

Similar to the N-Turku samples, the S-Turku rocks show a wide range both in major and minor element contents. One of the samples plots in the volcanic arc field in the Sr/Y vs Y and La/Yb vs Yb diagrams, while the other thirteen samples plot in the adakite/TTG field (Fig. 9). Half of the analyses show quite low Sr/Y ratios, the lowest of all the samples in this study. This depends mainly on the low Sr contents as the Y contents are systematically below 18ppm. Many of these rocks also tend to show negative Sr anomalies, in contrast to those in the N-Turku area (Fig. 10). In the La/Yb vs Yb diagram, all but one plot within the adakite/TTG-field. The relatively low Sr contents as well as the negative Sr and Eu anomalies suggest that plagioclase either remained in the source or, alternatively, was fractionated from the magma before emplacement. However, except for these discrepancies the S-Turku samples show similar intermediate compositions to the N-Turku samples, making our interpretation the same, *i.e.*, they are crustal melts but some bear signatures of the mantle through mixing processes.

Depth of melting

The position of nearly all the samples and, in particular, the Uki trondhjemites and tonalites, in the adakitic and TTG-fields in Figure 9 supports deep melting, where plagioclase was unstable and entered the melt phase together with Sr, while garnet was stable retaining Yb and Y. In many cases, crustal melting at pressures higher than 15kbar is suggested for reaching adakitic Sr/Y (and La/Yb) ratios, assuming constant contents of Sr and REE in the mafic crustal source lithologies (Moyen, 2009). However, Moyen (2009) showed that not only the pressure, but also the source composition has a drastic effect on the ratios of these elements in a magma. For example, high Sr/Y in the source leads to still higher ratios in the magma even at

moderate pressures. This effect is accentuated if the source contains an aluminous metasedimentary component. Melting of peraluminous sources may leave garnet in the residue at pressures as low as 5-6kbars, which can lead to adakitic Sr/Y ratios, but other geochemical characteristics of such rocks are not adakitic. It has been shown that garnet may be a stable residual phase during melting of amphibolitic sources from *c.* 10kbar and upwards (*e.g.*, Wolf and Willie, 1994; Skjerlie & Johnston, 1996). This can be regarded as the lower pressure limit for adakite formation from amphibolitic sources.

The range of ages of the inherited zircons in the *c.* 1.87Ga intrusions (Väisänen *et al.*, 2002 and this study), clearly indicates that mafic meta-igneous rocks in the crust cannot be the only source for the synorogenic magmatism, but that a sedimentary source must be involved. This seriously questions the deep melting region as a source for these rocks. However, based on the high ϵ_{Nd} values discussed above, the sedimentary component cannot be very large. Therefore, it is highly improbable that garnet crystallizing at shallow depths contributed to the elevated Sr/Y ratios. In addition, other geochemical features of the rocks in this study do not favour sedimentary protoliths (*e.g.*, the low K₂O/Na₂O; Fig. 7). In contrast, it is fully possible that the source, *i.e.*, a volcanic arc-type crust, already possessed relatively high Sr/Y, leading to even higher ratios by melting at moderate pressures, *i.e.*, in the middle crust.

Most of the the Uki trondhjemites and tonalites have Sr/Y ratios exceeding 100. These high ratios cannot be explained by source compositions alone and indicate deep melting in the presence of garnet. If a normal crustal Sr/Y ratio of 15 (Taylor and McLennan, 1985) is assumed in the source, a ratio of >300 requires 15kbar pressures (Moyen, 2009). Two trondhjemite samples are close to and five samples are much above that value (Fig. 8E). Therefore, even accepting a high Sr/Y source, high pressures are required, *i.e.*, pressures of the lower crust, at least for those rocks with the highest ratios. Samples from N-Turku show a wide scatter of Sr/Y, but in this area many of the rocks probably are hybrids between mantle- and crustal-derived magmas as previously discussed. The lowest Sr/Y values are encountered in the S-Turku samples, which might indicate the shallowest melting region or lowest Sr/Y in the source. A component of hybridization with low Sr/Y mafic rocks is most probably included also here.

Tectonic setting

The Svecofennian orogen, which constitutes a major part of the Fennoscandian Shield, is considered to have formed through successive episodic pulses in several phases. The first one was the accretionary Fennian orogeny at

c. 1.92–1.87Ga, during which the first volcanic arcs collided with the Archaean craton and then against each other (Lahtinen *et al.*, 2005). According to Lahtinen *et al.* (2005) an intervening extensional period, at *c.* 1.86–1.84Ga, was followed by a continent–continent collision between Fennoscandia and the Volgo–Sarmatian crustal block from the SE at 1.84–1.79Ga, which reworked the crust in southern Finland and central Sweden (Svecofennian orogeny). All in all, these two main orogenic cycles, complemented by magmatic additions from the mantle (Lahtinen *et al.*, 2009b), created an orogen that is one of the thickest in the Palaeoproterozoic (Windley, 1995). Even today it is *c.* 60km thick in the central parts and 50km thick in southern Finland and central Sweden. Prior to exhumation and erosion, the Svecofennian orogen was *c.* 70km thick (Korja *et al.*, 1993). Based on the present thick crust in the central Svecofennian arc complex, an area that more or less escaped the Svecofennian stage, it is assumed that the great thickness of the Svecofennian crust was reached already during its accretional stage by *c.* 1.87Ga, at least in the central Svecofennian arc complex (*e.g.*, Nironen *et al.*, 2000).

The volcanic arcs in southern Finland, the Uusimaa and Häme belts that form the southern Svecofennian arc complex, were formed between *c.* 1.90 and 1.88Ga and accreted and collided against the central Svecofennian arc complex at *c.* 1.87Ga (Väisänen *et al.*, 2002). On the basis of published and new (this study) single zircon age determinations, it is shown that the *c.* 1.87Ga magmatism is more widespread than previously thought, since many of these rocks appear to contain zircon populations of variable ages that in conventional geochronology yielded mixed ages. This magmatism comprises both mantle (mafic) and crustal (felsic) components, and their magmatic hybrids. The mantle part (diorites) shows elevated LILE and REE contents (compared to oceanic arc magmas), but has subduction-related signatures. A similar *c.* 1.87Ga mafic–felsic rock association with mantle-derived high-potassium mafic rocks and high Sr/Y felsic crustal melts has been described from Puutsaari in the eastern part of the southern Svecofennian arc complex in Russian Karelia (Konopelko and Eklund, 2003). There, rocks are coeval and mingle and mix with each other forming hybrids. Adakite-like rocks have also been described from the same region (Mattila, 2003). Early Svecofennian metamorphism and anatexis at 1.87–1.86Ga have also been reported in Sweden (Andersson *et al.*, 2004a, 2006b; Hermansson *et al.*, 2008; Högdahl *et al.*, 2008).

Because arc accretion had thickened the crust, probably assisted by magmatism from ongoing subduction, newly formed crustal melts obtained adakite- and TTG-like compositions by melting of garnet-bearing basaltic sources. Crustal melting took place during the final stage of arc accretion and crustal thickening or immediately after

that, before subsequent extension thinned the crust. Since the crustal melts are associated with coeval mantle-derived mafic magmatism, it is plausible that the mafic magmatism provided the heat source for crustal melting (*c.f.*, Andersson, 1991; Konopelko and Eklund, 2003).

Adakite-like crust-derived magmatism is not widely described from the Palaeoproterozoic Era. It is probably a common magma type in the Svecofennian orogen, where tectonic movements and magmatism thickened the crust to one of the thickest in the Palaeoproterozoic Era, similar to present-day Tibet (*e.g.*, Chung *et al.*, 2003; Hou *et al.*, 2004). It is likely that similar magma types occur in many Paleoproterozoic orogens that were subjected to thickening, either through arc accretion, magmatism or continental collision, provided that an appropriate heat source was available.

SUMMARY AND CONCLUSIONS

The recent single zircon age data suggest that the synorogenic magmatism in southern Finland occurred between *c.* 1875Ma and 1860Ma with most of the ages around 1.87Ga. Both mafic (1872±3Ma diorite) and felsic (1867±4Ma trondhjemite) magmatism dated in the present study belong to the 1.87Ga synorogenic magmatic group. Within analytical uncertainty, they are coeval, but combined with previously published ages also allow the interpretation that part of the mafic magmatism occurred slightly earlier than the felsic magmatism. The onset of the late-Svecofennian metamorphism is now extended back to *c.* 1.84Ga, as shown by zircon rims in the trondhjemite. The trondhjemite also contained inherited Archaean and Palaeoproterozoic zircons.

All evidences indicate that the *c.* 1.87Ga magmatism in SW Finland stems from two principally different sources: one in the mantle and the other in the mafic lower crust. The mantle component is represented by the mafic–intermediate Uki diorites that were derived from a mantle wedge source that was slightly enriched during a preceding subduction event. The crustal sources mostly consisted of juvenile (<2.1Ga) mafic arc crust, which by melting yielded typical adakite/TTG-like magmas. Intrusion of the mantle-derived magmas into the arc crust may have been the engine in the generation of the crustal melts. Most of the intermediate compositions represent mixtures between these two end members.

The crustal part of the synorogenic magmatism is expressed by the most felsic rocks among the trondhjemites and tonalites, while most tonalites, granodiorites and quartz diorites represent hybrids with the mantle-derived magmas. The Sr/Y and La/Yb ratios are adakite- and TTG-like, indicating that the crustal melts were derived from the

lower, mafic part of the thick Svecofennian arc crust. The Uki trondhjemites show the highest ratios, indicating the deepest source (pressure >15kbar). By the same reasoning the N-Turku rocks might have been derived from a slightly shallower melting region and the S-Turku rocks have the shallowest crustal source, with only half of the analysed rocks showing adakite/TTG-like Sr/Y ratios.

It is proposed that the arc accretion at *c.* 1.92-1.87Ga, combined with magmatic underplating into the lower crust, thickened the crust so that melting of the lower crust yielded adakite- and TTG-like compositions.

ACKNOWLEDGMENTS

The Laboratory for Isotope Geology at the Swedish Museum of Natural History provided funding, facilities and guidance for Sm-Nd analyses via SYNTHESYS (project SE TAF 2050), organized by European Community – Research Infrastructure Action (FP6 programme: Structuring the European Research Area). Maria Fischerström, Kjell Billström and Hans Schöberg helped in numerous ways with analyses. Martin Whitehouse, Chris Kirkland, Lev Ilyinsky and Kerstin Lindén at the NordSIM Laboratory are thanked for the help with the SIMS zircon dating. The NordSIM Laboratory is financed and operated under an agreement between the research councils of Denmark, Norway and Sweden, the Geological Survey of Finland and the Swedish Museum of Natural History. This study was funded by the Academy of Finland (project 117311), Ella and Georg Ehrnrooth Foundation, the Geological Survey of Finland, Suomen Tiedeseura Sohlbergin Delegaatio and the Turku University Foundation. We thank Elis Hoffmann and Ian Williams for very helpful reviews. This is NordSIM publication No. 310.

REFERENCES

- Allen, R.L., Lundström, I., Ripa, M., Simeonov, A., Christofferson, H., 1996. Facies analysis of a 1.9 Ga, continental margin, back-arc, felsic caldera province with diverse Zn-Pb-Ag-(Cu-Au) sulfide and Fe oxide deposits, Bergslagen region, Sweden. *Economic Geology*, 91, 979-1008.
- Andersen, T., Andersson, U.B., Graham, S., Åberg, G., Simonsen, S.L. 2009. Granitic magmatism by melting of juvenile continental crust: New constraints on the source of Palaeoproterozoic granitoids in Fennoscandia from Hf isotopes in zircon. *London, Journal of the Geological Society*, 166, 233-247.
- Andersson, U.B., 1991. Granitoid episodes and mafic-felsic magma interaction in the Svecofennian of the Fennoscandian shield, with main emphasis on the ~1.8Ga plutonics. *Precambrian Research*, 51, 127-149.
- Andersson, U.B., Neymark, L.A., Billström, K. 2002. Petrogenesis of Mesoproterozoic (Subjotnian) rapakivi complexes of central Sweden: implications from U-Pb zircon ages, Nd, Sr and Pb isotopes. *Transactions of the Royal Society of Edinburgh, Earth Sciences*, 92, 201-228.
- Andersson, U.B., Högdahl, K., Sjöström, H., Bergman, S., 2004a. Magmatic, detrital, and metamorphic ages in metamorphic rocks from south-central Sweden. *GFF*, 126, 16-17.
- Andersson, U.B., Sjöström, H., Högdahl, K., Eklund, O., 2004b. The Transscandinavian Igneous Belt, evolutionary models. *Geological Survey of Finland, 37 (Special Paper)*, 104-112.
- Andersson, U.B., Eklund, O., Fröjdö, S., Konopelko, D., 2006a. 1.8Ga magmatism in the Fennoscandian Shield: lateral variations in subcontinental mantle enrichment. *Lithos*, 86, 110-136.
- Andersson, U.B., Högdahl, K., Sjöström, H., Bergman, S., 2006b. Multistage growth and reworking of the Palaeoproterozoic crust in the Bergslagen area, southern Sweden; evidence from U-Pb geochronology. *Geological Magazine*, 143, 679-697.
- Andersson, U.B., Rutanen, H., Johansson, Å., Mansfeld, J., Rimlä, A., 2007. Characterization of the Paleoproterozoic mantle beneath the Fennoscandian Shield: Geochemistry and isotope geology (Nd, Sr) of ~1.8 Ga mafic plutonic rocks from the Transscandinavian Igneous Belt in southeast Sweden. *International Geology Review*, 49, 587-625.
- Arth, J.G., Barker, F., Peterman, Z.E., Friedman, I., 1978. Geochemistry of the gabbro-diorite-tonalite-trondhjemite suite of southwestern Finland and its implication for the origin of tonalitic and trondhjemitic magmas. *Journal of Petrology*, 19, 289-316.
- Baker, J.H., Hellingwerf, R.H., Oen, I.S., 1988. Structure, stratigraphy, and ore-forming processes in Bergslagen: implications for the development of the Svecofennian of the Baltic shield. *Geologie en Mijnbouw*, 67, 121-138.
- Barker, F., 1979. Trondhjemite: definition, environment and hypothesis of origin. In: Barker, F. (ed.). *Trondhjemites, Dacites, and Related Rocks*. Amsterdam, Elsevier, 1-12.
- Bergman, S., Högdahl, K., Nironen, M., Ogenhall, E., Sjöström, H., Lundqvist, L., Lahtinen, R., 2008. Timing of Palaeoproterozoic intra-orogenic sedimentation in the central Fennoscandian Shield; evidence from detrital zircon in metasandstone. *Precambrian Research*, 161, 231-249.
- Bogdanova, S.V., Bingen, B., Gorbatshev, R., Kheraskova, T.N., Kozlov, V.I., Puchkov, V.N., Volozh, Y.A., 2008. The East European Craton (Baltica) before and during the assembly of Rodinia. *Precambrian Research*, 160, 23-45.
- Cagnard, F., Gapais, D., Barbey, P., 2007. Collision tectonics involving juvenile crust: the example of the southern Finnish Svecofennides. *Precambrian Research*, 154, 125-141.
- Chardon, D., Gapais, D., Cagnard, F., 2009. Flow of ultra-hot orogens: A view from the Precambrian, clues for the Phanerozoic. *Tectonophysics*, 477, 105-118.
- Chung, S.-L., Liu, D., Ji, J., Chu, M.-F., Lee, H.-Y., Wen, D.-J., Lo, C.-H., Lee, T.-Y., Qian, Q., Zhang, Q., 2003. Adakites from continental collision zones: Melting of thickened lower crust beneath southern Tibet. *Geology*, 31, 1021-1024.

- Claesson, S., 1987. Nd isotope data on 1.9-1.2 Ga old basic rocks and metasediments from the Bothnian basin, central Sweden. *Precambrian Research*, 35, 115-126.
- Claesson, S., Lundqvist, T., 1995. Origins and ages of Proterozoic granitoids in the Bothnian basin, central Sweden: isotopic and geochemical constraints. *Lithos*, 36, 115-140.
- Claesson, S., Huhma, H., Kinny, P.D., Williams, I.S., 1993. Svecofennian detrital zircon ages implications for the Precambrian evolution of the Baltic Shield. *Precambrian Research*, 64, 109-130.
- Colley, H., Westra, L., 1987. The volcano-tectonic setting and mineralisation of the early Proterozoic Kemiö-Orijärvi-Lohja belt, SW Finland. *Geological Society of London*, 33 (Special Publications), 95-107.
- Condie, K., 2005. TTGs and adakites: are they both slab melts? *Lithos*, 80, 33-44.
- Defant, M.J., Drummond, M.S., 1990. Derivation of some modern arc magmas by melting of young subducted lithosphere. *Nature*, 347, 662-665.
- De Paolo, D.J., 1981. Neodymium isotopes in the Colorado Front Range and crust-mantle evolution in the Proterozoic. *Nature*, 291, 193-196.
- Ehlers, C., Lindroos, A., Jaanus-Järkkälä, M., 1986. Stratigraphy and geochemistry in the Proterozoic mafic volcanic rocks of the Nagu-Korpo area, SW Finland. *Precambrian Research*, 32, 307-318.
- Ehlers, C., Lindroos, A., Selonen, O., 1993. The late Svecofennian granite-migmatite zone of southern Finland - a belt of transpressive deformation and granite emplacement. *Precambrian Research*, 64, 295-309.
- Ehlers, C., Skiöld, T., Vaasjoki, M., 2004. Timing of Svecofennian crustal growth and collisional tectonics in Åland, SW Finland. *Bulletin of the Geological Society of Finland*, 76, 63-91.
- Gaál, G., Gorbatshev, R., 1987. An outline of the Precambrian evolution of the Baltic shield. *Precambrian Research*, 35, 15-52.
- Halla, J., van Hunen, J., Heilimo, E., Hölttä, P., 2009. Geochemical and numerical constraints on Neoarchean plate tectonics. *Precambrian Research*, 174, 155-162.
- Helenius, E.-M., Eklund, O., Väisänen, M., Hölttä, P., 2004. Petrogenesis of charnockites in the Turku granulite area. *Institute of Seismology, University of Helsinki, S-45 (Report)*, 17-20.
- Hermansson, T., Stephens, M.B., Corfu, F., Andersson, J., Page, L.M., 2007. Penetrative ductile deformation and amphibolite-facies metamorphism prior to 1851 Ma in the western part of the Svecofennian orogen, Fennoscandian Shield. *Precambrian Research*, 153, 29-45.
- Hermansson, T., Stephens, M.B., Corfu, F., Page, L.M., Andersson, J., 2008. Migratory tectonic switching, western Svecofennian orogen, central Sweden: Constraints from U/Pb zircon and titanite geochronology. *Precambrian Research*, 161, 250-278.
- Hietanen, A., 1943. Über das Grundgebirge des Kalantigebietes im südwestlichen Finnland. *Bulletin de la Commission géologique de Finlande*, 130, 106pp.
- Hietanen, A., 1947. Archaean geology of the Turku district in southwestern Finland. *Bulletin of the Geological Society of America*, 58, 1019-1084.
- Hildreth, W., Moorbath, S., 1988. Crustal contributions to arc magmatism in the Andes of central Chile. *Contributions to Mineralogy and Petrology*, 98, 455-489.
- Högdahl, K., Sjöström, H., 2001. Evidence for 1.82 Ga transpressive shearing in a 1.85 Ga granitoid in central Sweden: implications for the regional evolution. *Precambrian Research*, 105, 37-56.
- Högdahl, K., Sjöström, H., Andersson, U.B., Ahl, M., 2008. Continental margin magmatism and migmatization in the west-central Fennoscandian Shield. *Lithos*, 102, 435-459.
- Högdahl, K., Sjöström, H., Bergman, S., 2009. Ductile shear zones related to crustal shortening and domain boundary evolution in the central Fennoscandian Shield. *Tectonics*, 28, TC1003, 18pp. doi: 10.1029/2008TC002277
- Hou, Z.-Q., Gao, Y.-F., Qu, X.-M., Rui, Z.-Y., Mo, X.-X., 2004. Origin of adakitic intrusives generated during mid-Miocene east-west extension in southern Tibet. *Earth and Planetary Science Letters*, 220, 139-155.
- Huang, X.-L., Xu, Y.-G., Lan, J.-B., Yang, Q.-J., Luo, Z.-Y., 2009. Neoproterozoic adakitic rocks from Mopanshan in the western Yangtze Craton: Partial melts of a thickened lower crust. *Lithos*, 112, 367-381.
- Huhma, H., 1986. Sm-Nd, U-Pb and Pb-Pb isotopic evidence for the origin of the Early Proterozoic Svecokarelian crust in Finland. *Geological Survey of Finland*, 337 (Bulletin), 48pp.
- Huhma, H., 1987. Provenance of early Proterozoic and Archean metasediments in Finland: a Sm-Nd isotopic study. *Precambrian Research*, 35, 127-143.
- Jacobsen, S.B., Wasserburg, G.J., 1984. Sm-Nd isotopic evolution of chondrites and achondrites II. *Earth and Planetary Science Letters*, 6, 137-150.
- Jahn, B.M., Glikson, A.Y., Peucat, J.-J., Hickman, A.H., 1981. REE geochemistry and isotope data of Archaean silicic volcanics and granitoids from the Pilbara Block, western Australia: implications for the early crustal evolution. *Geochimica Cosmochimica Acta*, 45, 1633-1652.
- Janoušek, V., Farrow, G., Erban, V., 2006. Interpretation of whole-rock geochemical data in igneous geochemistry: Introducing Geochemical Data Toolkit (GCDKit). *Journal of Petrology*, 47, 1255-1259.
- Johannes, W., Ehlers, C., Kriegsman, L.M., Mengel, K., 2003. The link between migmatites and S-type granites in the Turku area, southern Finland. *Lithos*, 68, 69-90.
- Johansson, Å., 2009. Baltica, Amazonia and the SAMBA connection - 1000 million years of neighbourhood during the Proterozoic? *Precambrian Research*, 175, 221-234.
- Jurvanen, T., Eklund, O., Väisänen, M., 2005. Generation of A-type granitic melts during the late Svecofennian metamorphism in southern Finland. *GFF*, 127, 139-147.
- Kähkönen, Y., 2005. Svecofennian supracrustal rocks. In: Lehtinen, M., Nurmi, P.A., Rämö, O.T. (eds.). *Precambrian*

- Geology of Finland - Key to the Evolution of the Fennoscandian Shield. Amsterdam, Developments in Precambrian Geology, Elsevier, 14, 343-405.
- Kamber, B.S., Ewart, A., Collerson, K.D., Bruce, M.C., McDonald, G.D., 2002. Fluid-mobile trace element constraints on the role of slab melting and implications for Archean crustal growth models. *Contributions to Mineralogy and Petrology*, 144, 38-56.
- Kirkland, C.L., Daly, J.S., Whitehouse, M.J., 2008. Basement-cover relationships of the Kalak Nappe Complex, Arctic Norwegian Caledonides and constraints on Neoproterozoic terrane assembly in the North Atlantic region. *Precambrian Research*, 160, 245-276.
- Konopelko, D., Eklund, O., 2003. Timing and geochemistry of potassic magmatism in the eastern part of the Svecofennian domain, NW Ladoga Lake Region, Russian Karelia. *Precambrian Research*, 120, 37-53.
- Korja, A., Korja, T., Luosto, U., Heikkinen, P., 1993. Seismic and geoelectric evidence for collisional and extensional events in the Fennoscandian Shield - implications for Precambrian crustal evolution. *Tectonophysics*, 219, 129-152.
- Korja, A., Lahtinen, R., Nironen, M., 2006. The Svecofennian orogen: a collage of microcontinents and island arcs. *London, Geological Society*, 32 (Memoirs), 561-578.
- Korsman, K., Hölttä, P., Hautala, T., Wasenius, P., 1984. Metamorphism as an indicator of evolution and structure of the crust in eastern Finland. *Geological Survey of Finland*, 328 (Bulletin), 40pp.
- Korsman, K., Koistinen, T., Kohonen, J., Wennerström, M., Ekdahl, E., Honkamo, M., Edman, H., Pekkala, Y., 1997. Bedrock map of Finland 1:1 000 000. *Geological Survey of Finland*.
- Korsman, K., Korja, T., Pajunen, M., Virransalo, P., GGT/SVEKA Working Group, 1999. The GGT/SVEKA transect: structure and evolution of the continental crust in the Paleoproterozoic Svecofennian orogen in Finland. *International Geology Review*, 41, 287-333.
- Kurhila, M., Vaasjoki, M., Mänttari, I., Rämö, T., Nironen, M., 2005. U-Pb ages and Nd isotope characteristics of the lateorogenic, migmatizing microcline granites in southwestern Finland. *Bulletin of the Geological Society of Finland*, 77, 105-128.
- Kurhila, M., Andersen, T., Rämö, O.T., 2010. Diverse sources of crustal granitic magma: Lu-Hf isotope data on zircon in three Paleoproterozoic leucogranites of southern Finland. *Lithos*, 115, 263-271.
- Lahtinen, R., 1994. Crustal evolution of the Svecofennian and Karelian domains during 2.1–1.79 Ga, with special emphasis on the geochemistry and origin of 1.93–1.91 Ga gneissic tonalites and associated supracrustal rocks in the Rautalampi area, central Finland. *Geological Survey of Finland*, 378 (Bulletin), 128pp.
- Lahtinen, R., Huhma, H., 1997. Isotopic and geochemical constraints on the evolution of the 1.93–1.79 Ga Svecofennian crust and mantle. *Precambrian Research*, 82, 13-34.
- Lahtinen, R., Huhma, H., Kähkönen, Y., Mänttari, I., 2009a. Paleoproterozoic sediment recycling during multiphase orogenic evolution in Fennoscandia, the Tampere and Pirkanmaa belts, Finland. *Precambrian Research*, 174, 310-336.
- Lahtinen, R., Korja, A., Nironen, M., 2005. Paleoproterozoic tectonic evolution of the Fennoscandian Shield. In: Lehtinen, M., Nurmi, P.A., Rämö, O.T. (eds.). *The Precambrian Bedrock of Finland – Key to the Evolution of the Fennoscandian Shield*. Amsterdam, Elsevier Science B.V., 418-532.
- Lahtinen, R., Korja, A., Nironen, M., Heikkinen, P., 2009b. Paleoproterozoic accretionary processes in Fennoscandia. *Geological Society of London*, 318 (Special Publications), 237-256.
- Ludwig, K.R., 2003. User's Manual for Isoplot 3.00. A Geochronological Toolkit for Microsoft Excel. Berkeley Geochronology Center, 4 (Special Publications), 1-70.
- Lundström, I., Allen, R.L., Persson, P.-O., Ripa, M., 1998. Stratigraphies and depositional ages of Svecofennian, Paleoproterozoic metavolcanic rocks in E. Svealand and Bergslagen, south central Sweden. *GFF*, 120, 315-320.
- Macpherson, C.G., Dreher, S., Thirlwall, M.F., 2006. Adakites without slab melting: high pressure differentiation of island arc magma, Mindanao, the Philippines. *Earth and Planetary Science Letters*, 243, 581-593.
- Mansfeld, J., Beunk, F.F., Barling, J., 2005. 1.83-1.82 Ga formation of a juvenile volcanic arc – implications from U-Pb and Sm-Nd analyses of the Oskarshamn-Jönköping Belt, southeastern Sweden. *GFF*, 127, 149-157.
- Martin, H., 1999. The adakitic magmas: modern analogues of Archean granitoids. *Lithos*, 46, 411-429.
- Martin, H., Smithies, R.H., Rapp, R.P., Moyen, J.-F., Champion, D.C., 2005. An overview of adakite, tonalite-trondhjemite-granodiorite (TTG) and sanukitoid: relationships and some implications for crustal evolution. *Lithos*, 79, 1-24.
- Martins, G., Oliveira, E.P., Lafon, J.M., 2009. The Algodões amphibolite-tonalite gneiss sequence, Borborema Province, NE Brazil: Geochemical and geochronological evidence for Paleoproterozoic accretion of oceanic plateau/back-arc basalts and adakitic plutons. *Gondwana Research*, 15, 71-85.
- Mattila, J., 2004. Geochemical and Sm-Nd isotopic constraints on the crustal evolution of the Kitee-Lahdenpohja area, southeastern Finland and northwestern Russia. M.Sc. Thesis. University of Turku, 102pp.
- Middlemost, E.A.K., 1994. Naming materials in the magma/igneous rock system. *Earth-Science Reviews*, 37, 215-224.
- Mouri, H., Väisänen, M., Huhma, H., Korsman, K., 2005. Sm-Nd garnet and U-Pb monazite dating of high-grade metamorphism and crustal melting in the West Uusimaa area, southern Finland. *GFF*, 127, 123-128.
- Moyen, J.-F., 2009. High Sr/Y and La/Yb ratios: The meaning of the "adakitic signature". *Lithos*, 112, 556-574.
- Muir, R.J., Weaver, S.D., Bradshaw, J.D., Eby, G.N., Evans, J.A., 1995. *Geochemistry of the Cretaceous Separation Point Batholith, New Zealand: granitoid magmas formed*

- by melting of mafic lithosphere. *Journal of the Geological Society London*, 152, 689-701.
- Ogenhall, E., 2007. Plate tectonic settings of the Svecofennian Palaeoproterozoic volcanic rocks at Hamrånge and Loos, south central Sweden, based on geochemical data. *GFF*, 129, 211-226.
- Nironen, M., 1997. The Svecofennian Orogen: a tectonic model. *Precambrian Research*, 86, 21-44.
- Nironen, M., 1999. Structural and magmatic evolution in the Loimaa area, southwestern Finland. *Bulletin of the Geological Society of Finland*, 71, 57-71.
- Nironen, M., Elliott, B.A., Rämö, O.T., 2000. 1.88-1.87 Ga post-kinematic intrusions of the Central Finland Granitoid Complex: a shift from C-type to A-type magmatism during lithospheric convergence. *Lithos*, 53, 37-58.
- Nironen, M., Kurhila, M., 2008. The Veikkola granite area in southern Finland: emplacement of a 1.83-1.82 Ga plutonic sequence in an extensional regime. *Bulletin of the Geological Society of Finland*, 80, 39-68.
- Pajunen, M., Airo, M.-L., Elminen, T., Mänttari, I., Niemelä, R., Vaarma, M., Wasenius, P., Wennerström, M., 2008. Tectonic evolution of the Svecofennian crust in southern Finland. *Geological Survey of Finland*, 47 (Special Paper), 15-160.
- Patchett, P.J., Gorbatshev, R., Todt, W., 1987. Origin of continental crust of 1.9-1.7 Ga age. Nd isotopes in the Svecofennian orogenic terrains of Sweden. *Precambrian Research*, 35, 145-160.
- Patchett, J., Kouvo, O., 1986. Origin of continental crust of 1.9-1.7 Ga age: Nd isotopes and U-Pb zircon ages in the Svecofennian terrain of South Finland. *Contributions to Mineralogy and Petrology*, 92, 1-12.
- Pearce, J.A., 1996. A user's guide to basalt discrimination diagrams. In: Wyman, D.A. (ed.). *Trace Element Geochemistry of Volcanic Rocks: Applications for Massive Sulphide Exploration*. Geological Association of Canada, Short Course Notes, 12, 79-113.
- Peccerillo, R., Taylor, S.R., 1976. Geochemistry of Eocene calc-alkaline volcanic rocks from the Kastamonu area, northern Turkey. *Contributions to Mineralogy and Petrology*, 58, 63-81.
- Pin, C., Zalduegui, J.F.S., 1997. Sequential separation of light rare-earth elements, thorium and uranium by miniaturized extraction chromatography: Application to isotopic analyses of silicate rocks. *Analytica Chimica Acta*, 339, 79-89.
- Rämö, O.T., Vaasjoki, M., Mänttari, I., Elliott, B.A., Nironen, M., 2001. Petrogenesis of the post-kinematic magmatism of the Central Finland Granitoid Complex I; radiogenic isotope constraints and implications for crustal evolution. *Journal of Petrology*, 42, 1971-1993.
- Richards, J.R., Kerrich, R., 2007. Adakite-like rocks: Their diverse origins and questionable role in metallogenesis. *Economic Geology*, 102 (Special Paper), 537-576.
- Romer, R.L., Öhlander, B. 1995. Tectonic implications of an 1846±1 Ma old migmatitic granite in south-central Sweden. *GFF*, 117, 69-74.
- Rutanen, H., Andersson, U.B., 2009. Mafic plutonic rocks in a continental-arc setting: geochemistry of 1.87-1.78 Ga rocks from south-central Sweden and models of their palaeotectonic setting. *Geological Journal*, 44, 241-279.
- Rutanen, H., Andersson, U.B., Väisänen, M., Johansson, Å., Fröjdö, S., Lahaye, Y., Eklund, O., 2011. 1.8 Ga magmatism in southern Finland: strongly enriched mantle and juvenile crustal sources in a post-collisional setting. *International Geology Review*, 53, 1622-1683.
- Rutland, R.W.R., Williams, I.S., Korsman, K., 2004. Pre-1.91 Ga deformation and metamorphism in the Palaeoproterozoic Vammala Migmatite Belt, southern Finland, and implications for Svecofennian tectonics. *Bulletin of the Geological Society of Finland*, 76, 93-140.
- Selonen, O., Ehlers, C., 1998. Structural observations on the Uusikaupunki trondjemite sheet, SW Finland. *GFF*, 120, 379-382.
- Sheppard, S., Griffin, T.J., Tyler, I.M., Page, R.W., 2001. High- and low-K granites and adakites at a Palaeoproterozoic plate boundary in northwestern Australia. *Journal of the Geological Society*, 158, 547-560.
- Skjerlie, K.P., Johnston, A.D., 1996. Vapour-absent melting from 10 to 20 kbar of crustal rocks that contain multiple hydrous phases: implications for anatexis in the deep to very deep continental crust and active continental margins. *Journal of Petrology*, 37, 661-691.
- Skyttä, P., Mänttari, I., 2008. Structural setting of late Svecofennian granites and pegmatites in Uusimaa Belt, SW Finland: Age constraints and implications for crustal evolution. *Precambrian Research*, 164, 86-109.
- Skyttä, P., Väisänen, M., Mänttari, I., 2006. Preservation of Palaeoproterozoic early Svecofennian structures in the Orijärvi area, SW Finland – Evidence for polyphase strain partitioning. *Precambrian Research*, 150, 153-172.
- Smithies, R.H., 2000. The Archaean tonalite-trondjemite-granodiorite (TTG) series is not an analogue of Cenozoic adakite. *Earth and Planetary Science Letters*, 182, 115-125.
- Stacey, J.S., Kramers, J.D., 1975. Approximation of terrestrial lead isotope evolution by a two-stage model. *Earth and Planetary Science Letters*, 26, 207-221.
- Steiger, R.H., Jäger, E., 1977. Subcommittee on geochronology: convention on the use of decay constants in geo- and cosmochronology. *Earth and Planetary Science Letters*, 36, 359-362.
- Stephens, M.B., Ripa, M., Lundström, I., Persson, L., Bergman, T., Ahl, M., Wahlgren, C.-H., Persson, P.-O., Wickström, L., 2009. Synthesis of the bedrock geology in the Bergslagen region, Fennoscandian Shield, south-central Sweden. *Sveriges geologiska undersökning*, 58, 260pp.
- Sun, S.-S., McDonough, W.F., 1989. Chemical and isotopic systematics of oceanic basalts: implications for mantle composition and processes. *Geological Society of London*, 42 (Special Publications), 313-345.
- Suominen, V., 1991. The chronostratigraphy of southwestern Finland with special reference to Postjotnian and Subjotnian

- diabases. Geological Survey of Finland, 356 (Bulletin), 100pp.
- Suominen, V., Fagerström, P., Torssonen, M., 1994. Geological map of Finland 1:100 000. Pre-Quaternary rocks, Uusikaupunki. Espoo, Geological Survey of Finland, Sheet 1131.
- Suominen, V., Fagerström, P., Torssonen, M., 2006. Geological Map of Finland 1:100 000, Explanation to the maps of Pre-Quaternary rocks, Uusikaupunki (in Finnish with English Summary). Espoo, Geological Survey of Finland, Sheet 1131, 89pp.
- Talikka, M., Mänttari, I., 2005. Pukala intrusion, its age and connection to hydrothermal alteration in Orivesi, southwestern Finland. Bulletin of the Geological Society of Finland, 77, 165-180.
- Taylor, S.R., McLennan, S.M., 1985. The continental crust: its composition and evolution. Geoscience texts. Oxford, Blackwell, 312pp.
- Torvela, T., Ehlers, C., 2010. From ductile to brittle deformation: structural development and strain distribution along a crustal-scale shear zone in SW Finland. International Journal of Earth Sciences, 99, 1133-1152.
- Torvela, T., Mänttari, I., Hermansson, T., 2008. Timing of deformation phases within the South Finland shear zone, SW Finland. Precambrian Research, 160, 277-298.
- Vaasjoki, M., Huhma, H., Lahtinen, R., Vestin, J., 2003. Sources of Svecofennian granitoids in the light of ion probe U-Pb measurements on their zircons. Precambrian Research, 121, 251-262.
- Väisänen, M., Hölttä, P., 1999. Structural and metamorphic evolution of the Turku migmatite complex, southwestern Finland. Bulletin of the Geological Society of Finland, 71, 177-218.
- Väisänen, M., Kirkland, C.L., 2008. U-Th-Pb geochronology of igneous rocks in the Toija and Salittu Formations, Orijärvi area, southwestern Finland: Constraints on the age of volcanism and metamorphism. Bulletin of the Geological Society of Finland, 80, 73-87.
- Väisänen, M., Mänttari, I., 2002. 1.90-1.88 Ga arc and back-arc basin in the Orijärvi area, SW Finland. Bulletin of the Geological Society of Finland, 74, 185-214.
- Väisänen, M., Mänttari, I., Hölttä, P., 2002. Svecofennian magmatic and metamorphic evolution in southwestern Finland as revealed by U-Pb zircon SIMS geochronology. Precambrian Research, 116, 111-127.
- Väisänen, M., Skyttä, P., 2007. Late Svecofennian shear zones in southwestern Finland. GFF, 129, 55-64.
- Väisänen, M., Westerlund, G., 2007. Palaeoproterozoic mafic and intermediate metavolcanic rocks in the Turku area, SW Finland. Bulletin of the Geological Society of Finland, 79, 127-141.
- Valbracht, J., Oen, I.S., Beunk, F.F., 1994. Sm-Nd isotope systematics of 1.9-1.8 Ga granites from western Bergslagen, Sweden: inferences on a 2.1-2.0 Ga crustal precursor. Chemical Geology, 112, 21-37.
- Van Duin, J.A., 1992. The Turku Granulite Area, SW Finland: a fluid-absent Svecofennian granulite occurrence. PhD. Thesis. Amsterdam (Holland), Vrije Universiteit, 234pp.
- Verma, S.P., Torres-Alvarado, I.S., Sotelo-Rodríguez, Z.T., 2002. SINCLAS: Standard igneous norm and volcanic rock classification system. Computers & Geosciences, 28, 711-715.
- Weihed, P., Arndt, N., Billström, K., Duchesne, J.-C., Eilu, P., Martinsson, O., Papunen, H., Lahtinen, R., 2005. Precambrian geodynamics and ore formation: the Fennoscandian Shield. Ore Geology Reviews, 27, 273-322.
- Whitehouse, M.J., Kamber, B.S., 2005. Assigning dates to thin gneissic veins in high-grade metamorphic terranes: a cautionary tale from Akilia, southwest Greenland. Journal of Petrology, 46, 291-318.
- Whitehouse, M.J., Kamber, B., Moorbath, S., 1999. Age significance of U-Th-Pb zircon data from early Archaean rocks of west Greenland – a reassessment based on combined ion-microprobe and imaging studies. Chemical Geology, 160, 201-224.
- Wiedenbeck, M., Allé, P., Corfu, F., Griffin, W.L., Meier, M., Oberli, F., von Quadt, A., Roddick, J.C., Spiegel, W., 1995. Three natural zircon standards for U-Th-Pb, Lu-Hf, trace element and REE analyses. Geostandards Newsletter, 19, 1-23.
- Williams, I.S., Rutland, R.W.R., Kousa, J., 2008. A regional 1.92 Ga tectonothermal episode in Ostrobothnia, Finland: implications for models of Svecofennian accretion. Precambrian Research, 165, 15-36.
- Wolf, M.B., Wyllie, P.J., 1994. Dehydration-melting of amphibolite at 10 kbar: the effects of temperature and time. Contributions to Mineralogy and Petrology, 115, 369-383.
- Windley, B.F., 1995. The Evolving Continents. Chichester, John Wiley & Sons, 3rd edition, 526pp.
- Zhang, S.-B., Zheng, Y.-F., Zhao, Z.-F., Wu, Y.-B., Yuan, H., Wu, F.-Y., 2009. Origin of TTG-like rocks from anatexis of ancient lower crust: Geochemical evidence from Neoproterozoic granitoids in South China. Lithos, 113, 347-368.

Manuscript received July 2010;
revision accepted October 2011;
published Online February 2012.

ELECTRONIC APPENDIX

TABLE 1 | Geochemical analyses from plutonic rocks in southwestern Finland

Sample	29-MJV-05	7-MJV-06	8-MJV-06	9-MJV-06	12-MJV-06	17-MJV-06	18-MJV-06	14-MJV-07
Sample area	Uki	Uki	Uki	Uki	Uki	Uki	Uki	Uki
N-coordinate ^a	6760730	6757382	6760936	6757319	6760538	6755771	6759462	6762618
E-coordinate ^a	3198231	3188554	3188212	3201716	3196381	3203586	3195227	3199695
Rock type ^b	Trond	Trond	Trond	Trond	Trond	Trond	Trond	Trond
Laboratory	Acme	Acme	Acme	Acme	Acme	Acme	Acme	Acme
SiO ₂	71.64	68.9	67.8	69.94	69.98	70.86	70.7	68.29
TiO ₂	0.22	0.34	0.42	0.34	0.26	0.27	0.22	0.37
Al ₂ O ₃	15.62	16.46	16.59	15.82	16.3	15.67	16.03	16.47
Fe ₂ O ₃	1.62	2.92	3.52	2.93	2.26	2.64	2.02	2.98
FeO	1.46	2.63	3.17	2.64	2.03	2.38	1.82	2.68
MnO	0.02	0.03	0.03	0.02	0.02	0.02	0.02	0.03
MgO	0.59	0.77	0.98	0.91	0.63	0.68	0.48	0.98
CaO	2.04	2.91	2.84	2.11	2.21	2.23	1.89	2.61
Na ₂ O	5.64	5.11	5.02	5.17	5.9	5.23	5.7	5.13
K ₂ O	1.46	1.41	1.62	1.66	1.62	1.6	2.07	1.97
P ₂ O ₅	0.07	0.07	0.09	0.09	0.06	0.08	0.08	0.108
Mg# ^c	42	34	36	38	36	34	32	39
Sc	2	4	4	5	2	3	2	3
Ba	264.4	228.7	324.8	132	386.6	169.9	452.4	470
Cs	1.2	4	4.4	3.3	1.6	3.9	1.8	3.4
Ga	21.5	21.5	20.4	21.3	23.6	20.4	21.7	22.3
Hf	3	4.3	4.4	3.6	3.5	4.2	3.3	3.9
Nb	1.6	4.5	3.8	4.9	1.4	5.3	1.4	4.3
Rb	34.7	50.3	62.8	64.5	40.3	78.5	52.1	64
Sr	923.3	676.2	606	658.8	987.3	361.1	960.6	645
Ta	<.1	0.5	0.3	0.4	0.1	0.6	0.2	0.2
Th	3.2	0.7	3.8	2.7	1.8	5.1	1.9	3.6
U	1.4	1	2.4	2.8	1.5	3.3	1.3	1.4
V	18	31	31	28	22	15	19	27
Zr	101.6	144.3	158.4	111.9	113.1	135.3	105.4	139.5
Y	2.5	2.4	8	2.3	2.7	2.6	2.6	3.7
La	12.9	4.8	20.1	9.9	9.3	14	9.2	17.1
Ce	24.5	8.6	36.6	18.1	18.6	25.5	17.6	31.5
Pr	3.63	1.08	4.08	1.99	2.15	2.78	2.12	3.54
Nd	10.7	3.7	15	6.6	7.2	9.6	8.6	12.9
Sm	1.9	0.7	2.5	1.1	1.5	1.6	1.5	2.16
Eu	0.71	0.51	0.71	0.58	0.46	0.45	0.4	0.7
Gd	1.04	0.46	2.08	0.64	0.97	1.02	1.11	1.35
Tb	0.15	0.11	0.37	0.11	0.14	0.16	0.12	0.19
Dy	0.65	0.4	1.49	0.48	0.6	0.6	0.64	0.79
Ho	0.09	0.09	0.25	0.08	<.05	0.06	0.07	0.13
Er	0.3	0.24	0.63	0.18	0.23	0.15	0.2	0.33
Tm	<.05	0.07	0.1	<.05	<.05	<.05	<.05	0.05
Yb	0.3	0.33	0.53	0.23	0.13	0.09	0.2	0.28
Lu	0.04	0.02	0.12	0.03	0.02	0.02	0.03	0.04
Cu	28.7	7.7	7.3	5.1	12.1	3.3	3.4	6
Pb	1.5	4	2.3	4.9	3.7	2	3.2	4.4
Zn	45	46	54	82	39	51	45	54
Cr	6.7	13.7	<6.8	<6.8	13.7	6.8	<6.8	<13.7
Ni	5	4.4	3.1	3.6	3.5	3.2	1.5	7.2
La/Yb	43	14.5	37.9	43	71.5	155.6	46	61.1
(La/Yb) _N ^d	30.8	10.4	27.2	30.9	51.3	111.6	33	43.8
Sr/Y	369	282	76	286	366	139	369	174

TABLE I | Continued

Sample	15-MJV-07	16-MJV-07	14-MJV-06	15-MJV-06	1-MJV-07	5-MJV-07	11-MJV-07	12-MJV-07
Sample area	Uki	Uki	Uki	Uki	Uki	Uki	Uki	Uki
N-coordinate ^a	6754069	6750815	6778973	6770031	6805958	6787427	6771224	6771547
E-coordinate ^a	3195439	3194941	3191229	3191569	3209255	3204396	3199318	3193640
Rock type ^b	Trond	Trond	Ton	Ton	Ton	Ton	Ton	Ton
Laboratory	Acme	Acme	Acme	Acme	Acme	Acme	Acme	Acme
SiO ₂	71.72	72.15	65.24	66.38	67.8	69.25	67.15	63.5
TiO ₂	0.18	0.19	0.6	0.43	0.59	0.44	0.56	0.61
Al ₂ O ₃	15.48	15.41	16.29	16.57	15.16	15.38	15.76	15.96
Fe ₂ O ₃	1.82	1.79	4.58	3.86	4.54	3.49	4.09	4.55
FeO	1.64	1.61	4.12	3.47	4.09	3.14	3.68	4.09
MnO	0.02	0.02	0.07	0.05	0.05	0.04	0.05	0.06
MgO	0.57	0.45	1.99	1.83	1.38	1.3	1.43	1.79
CaO	1.92	1.93	3.75	3.52	2.08	2.76	3.28	3.48
Na ₂ O	5.68	5.5	4.24	4.31	4.15	4.31	4.39	3.88
K ₂ O	1.8	2.25	1.91	1.92	2.63	1.91	1.93	2.39
P ₂ O ₅	0.048	0.052	0.4	0.14	0.259	0.161	0.211	0.313
Mg# ^c	38	33	46	48	38	42	41	44
Sc	3	2	6	6	9	6	6	7
Ba	344	395	440.1	560.5	296	443	567	532
Cs	2.4	4.2	3.6	7.2	5.9	4.3	7.7	9
Ga	22	21.4	21.9	22.9	18	20.6	21.8	21.9
Hf	2.1	2.4	4.3	4.3	6.7	3.4	4.1	4
Nb	1.9	1.7	8.3	6	21.5	6.5	8	10.2
Rb	48.7	54.2	69.6	80.9	120	99.2	77.3	78.3
Sr	912.4	885.3	1322.7	799.4	417	495	882.6	905.6
Ta	0.1	0.2	0.5	0.3	1	0.4	0.5	0.5
Th	1.6	0.3	5.8	5.8	7.5	4.9	4.5	4.8
U	0.5	0.6	4.1	4	4.1	2	1.8	2.3
V	20	14	67	57	50	49	59	94
Zr	74.8	81.4	153.9	146	310.6	132.1	154.1	159.6
Y	1.1	0.7	11.7	6.2	13.9	6.7	7.8	10.4
La	9.9	3.7	45.6	21.6	65.7	25	29.7	39.6
Ce	18.8	6.9	107.8	45.1	128.4	47.1	60.5	82.7
Pr	1.99	0.82	13.88	5.38	14.56	5.16	7.11	9.99
Nd	6.8	3.6	53.6	19.3	53.5	18.9	27.5	36.2
Sm	0.96	0.53	8.3	3	7.17	3.05	4.55	5.53
Eu	0.43	0.45	2.09	0.86	1.56	0.77	1.28	1.65
Gd	0.6	0.33	5.35	1.88	4.43	2.01	2.96	3.89
Tb	0.07	0.04	0.65	0.25	0.63	0.3	0.39	0.51
Dy	0.25	0.13	2.38	1.31	2.88	1.5	1.74	2.29
Ho	0.03	0.03	0.34	0.19	0.48	0.24	0.26	0.41
Er	0.08	<0.03	0.81	0.51	1.21	0.6	0.65	0.98
Tm	0.02	<0.01	0.14	0.08	0.19	0.08	0.09	0.16
Yb	0.09	0.08	0.69	0.45	1.09	0.52	0.59	0.77
Lu	0.02	0.01	0.1	0.06	0.2	0.09	0.08	0.17
Cu	6.2	4	26.1	15.7	10.8	25.1	15.4	13.7
Pb	2.3	2.1	4.4	4.8	7.8	4.7	4.3	4.8
Zn	49	41	57	56	91	64	71	79
Cr	<13.7	<13.7	13.7	38.5	<13.7	27.4	13.7	<13.7
Ni	4.3	3.8	8.1	23.7	7.4	12.8	12.2	20.9
La/Yb	110	46.3	66.1	48	60.3	48.1	50.3	51.4
(La/Yb) _N ^d	78.9	33.2	47.4	34.4	43.2	34.5	36.1	36.9
Sr/Y	829	1265	113	129	30	74	113	87

TABLE I | Continued

Sample	13-MJV-07	28-MJV-05	10-MJV-06	19-MJV-06	13-MJV-06	20-MJV-06	6-MJV-07	7-MJV-07
Sample area	Uki	Uki	Uki	Uki	Uki	Uki	Uki	Uki
N-coordinate ^a	6766670	6758277	6758482	6757178	6776573	6757918	6784705	6784398
E-coordinate ^a	3199053	3197083	3200453	3197354	3197454	3197405	3204216	3204195
Rock type ^b	Ton	Dr	Dr	Dr	Dr	Dr	Dr	Dr
Laboratory	Acme	Acme	Acme	Acme	Acme	Acme	Acme	Acme
SiO ₂	67.07	57.27	56.34	57.78	60.11	57.22	57.49	60.01
TiO ₂	0.46	0.87	0.91	0.82	0.69	0.88	0.86	0.77
Al ₂ O ₃	15.5	15.8	16.54	15.84	15.11	16.38	14.4	14.72
Fe ₂ O ₃	3.91	7.44	7.63	7.08	6.1	7.36	8.03	6.53
FeO	3.52	6.69	6.87	6.37	5.49	6.62	7.23	5.88
MnO	0.05	0.1	0.09	0.09	0.08	0.1	0.12	0.08
MgO	1.73	5.17	4.67	4.78	4.01	4.61	5.85	4.78
CaO	2.95	6.51	5.87	5.72	5.1	6.15	5.98	5.13
Na ₂ O	4.21	3.85	3.81	4.12	3.98	3.79	2.95	3.83
K ₂ O	1.55	1.7	2.15	1.4	3.18	2.09	2.21	2.57
P ₂ O ₅	0.13	0.43	0.33	0.33	0.47	0.39	0.496	0.458
Mg# ^c	47	58	55	57	57	55	59	59
Sc	7	16	15	15	11	16	20	14
Ba	305	369.6	433.9	284.1	692.7	448.2	402	449
Cs	5.7	4.5	2.3	4.8	5.7	2.8	3.6	4.3
Ga	20.6	20.8	22.1	20.4	20	20.1	18.9	17.8
Hf	3.6	2.7	3.8	6.8	5.6	4.7	3.7	4.1
Nb	4.8	7.2	8.1	7.6	11.5	8.1	19.3	15.2
Rb	65.1	44	56.4	35	97.4	54.8	142.3	117.6
Sr	691.9	915.6	796.5	741.6	1229	899.9	827.3	843.3
Ta	0.2	0.4	0.4	0.5	0.8	0.4	0.9	0.7
Th	4.7	5.7	7.7	4.7	13.9	6.4	10.6	7.3
U	1.7	2.9	2.8	3.2	4.3	3.3	4.1	2.6
V	48	150	140	159	105	133	150	109
Zr	116	90.9	124.4	227.5	194.4	155.6	148.4	155.3
Y	5.8	19.7	15.5	17.4	16.5	18.4	25.4	17.9
La	17.7	54.6	35.7	42.5	45.5	43.9	53.2	42.9
Ce	35.6	109.9	81.4	98.8	108.7	102.9	124.8	97.2
Pr	4.22	13.64	10.21	12.86	14.14	13.37	16.86	12.52
Nd	16.7	54.9	41.9	51.7	55.1	55	70.2	52.1
Sm	2.95	9.6	7	8.8	9.2	9.2	12.65	9.08
Eu	0.82	2.64	1.88	1.78	2.16	2.42	2.97	2
Gd	2.11	5.97	4.99	6.16	6.56	6.36	8.3	6.12
Tb	0.26	0.83	0.68	0.8	0.86	0.88	1.13	0.77
Dy	1.21	3.62	2.78	3.44	3.4	3.76	5.25	3.84
Ho	0.2	0.63	0.47	0.56	0.54	0.53	0.86	0.61
Er	0.54	1.67	1.28	1.4	1.26	1.38	2.3	1.57
Tm	0.07	0.15	0.21	0.23	0.25	0.21	0.36	0.23
Yb	0.49	1.45	1.09	1.27	1.1	1.34	2.1	1.47
Lu	0.08	0.19	0.23	0.23	0.19	0.24	0.3	0.22
Cu	5.1	51.3	41.6	42.1	45.8	41.2	46.6	51.6
Pb	3.5	1	2.7	1.9	4.1	3.9	14.5	5.2
Zn	62	38	55	46	47	57	89	65
Cr	34.2	143.7	143.7	116.3	140.8	130	328.4	218.9
Ni	18.3	87	54.2	43.9	43.9	52.9	66.1	69.6
La/Yb	36.1	37.7	32.8	33.5	41.4	32.8	25.3	29.2
(La/Yb) _N ^d	25.9	27	23.5	24	29.7	23.5	18.2	20.9
Sr/Y	119	46	51	43	74	49	33	47

TABLE I | Continued

Sample	8-MJV-07	9-MJV-07	10-MJV-07	1-EMH-01	2-EMH-01	3A-EMH-01	3D-EMH-01	4-EMH-01
Sample area	Uki	Uki	Uki	N-Turku	N-Turku	N-Turku	N-Turku	N-Turku
N-coordinate ^a	6782966	6779431	6777185	6703544	6718937	6723270	6723270	6723172
E-coordinate ^a	3198702	3203796	3206809	3234043	3246011	3233356	3233356	3231862
Rock type ^b	Dr	Dr	Dr	Charn	Charn	Ton	Ton	Charn
Laboratory	Acme	Acme	Acme	ActLab	ActLab	ActLab	ActLab	ActLab
SiO ₂	61.08	59.43	60.69	69.5	63.94	64.92	65.8	62.96
TiO ₂	0.96	0.8	0.76	0.32	0.65	0.773	0.696	0.782
Al ₂ O ₃	15.02	15.78	15.35	16.95	17.36	15.41	15.93	15.54
Fe ₂ O ₃	6.64	6.49	6.3	1.29	4.81	5.76	5.01	5.8
FeO	5.97	5.84	5.67	1.16	4.33	5.18	4.51	5.22
MnO	0.08	0.09	0.08	0.014	0.046	0.065	0.061	0.069
MgO	4.25	4.21	4.17	0.79	1.88	2.84	2.19	2.99
CaO	4.7	5.33	5	3.78	3.17	3.9	4.04	4.84
Na ₂ O	2.84	4.07	3.75	5.02	5.3	3.42	3.7	4.32
K ₂ O	2.6	2.11	2.16	1.79	1.98	2.05	1.88	1.8
P ₂ O ₅	0.494	0.48	0.473	0.1	0.16	0.21	0.18	0.19
Mg# ^c	56	56	57	55	44	49	46	51
Sc	11	13	13	2	6	11	10	12
Ba	686	623	562	399	361	745	442	441
Cs	9.4	6.2	6.6	0.1	2.3	10.2	24.6	2.4
Ga	17.3	19.6	18.5	21	24	21	22	23
Hf	3.6	4.8	4.1	2.7	0.9	5.2	4.2	4.3
Nb	17.7	10.8	12.3	5.2	6.9	8	9.7	8.1
Rb	140.9	99.3	126.9	31	91	118	117	74
Sr	997.9	1192	1084	591	719	521	564	627
Ta	0.7	0.5	0.7	0.25	0.36	0.36	0.61	0.34
Th	6.3	5.6	7.7	0.53	0.14	5.47	7.79	1.44
U	2.4	2.5	3.6	0.46	0.37	2.03	3.18	0.3
V	92	115	110	16	57	86	71	87
Zr	147.6	189.2	164.2	102	28	196	152	160
Y	15.8	16.8	17.1	2.6	2.9	12.6	12	12.7
La	19.6	54.4	53	12.6	7.19	29.9	34	24.9
Ce	47.8	116.1	112.4	20.5	13.7	62.8	65.2	49.9
Pr	7.15	14.38	14.12	1.86	1.47	6.97	7.11	5.83
Nd	33.9	58.2	58	6.33	5.49	25.9	25	22.6
Sm	7.16	9.36	9.66	1.09	1.19	4.89	4.18	4.11
Eu	2.02	2.51	2.32	1.01	0.848	1.68	1.41	1.43
Gd	5.11	6.24	6.31	0.79	1.04	4.23	3.73	3.92
Tb	0.68	0.78	0.79	0.11	0.15	0.5	0.49	0.53
Dy	3.23	3.56	3.62	0.57	0.7	2.61	2.43	2.54
Ho	0.54	0.55	0.56	0.1	0.11	0.5	0.46	0.48
Er	1.41	1.46	1.5	0.25	0.24	1.3	1.26	1.31
Tm	0.22	0.2	0.23	0.03	0.018	0.153	0.158	0.166
Yb	1.33	1.27	1.35	0.25	0.17	1.04	0.96	1.02
Lu	0.19	0.19	0.2	0.041	0.022	0.166	0.15	0.157
Cu	26	17.4	20.2	<10	24	31		37
Pb	7.4	3.5	3.5	14	9	10	8	6
Zn	80	63	69	<30	85	73	65	63
Cr	164.2	130	136.8	<20	36	81	61	86
Ni	58	53.3	53.6	<20	<20	38	36	57
La/Yb	14.7	42.8	39.3	50.4	42.3	28.8	35.4	24.4
(La/Yb) _N ^d	10.6	30.7	28.2	36.2	30.3	20.6	25.4	17.5
Sr/Y	63	71	63	227	248	41	47	49

TABLE I | Continued

Sample	5AH-EMH-01	5B-EMH-01	6-EMH-01	110-MAV-02	111-MAV-02	112-MAV-02	113-MAV-02
Sample area	N-Turku	N-Turku	N-Turku	N-Turku	N-Turku	N-Turku	N-Turku
N-coordinate ^a	6721759	6721759	6715821	6727993	6727774	6745983	6747935
E-coordinate ^a	3228286	3228286	3226119	3238739	3236642	3260889	3266247
Rock type ^b	Charn	Charn	Charn	Ton	Ton	Grdr	Ton
Laboratory	ActLab	ActLab	ActLab	ActLab	Acme	Acme	Acme
SiO ₂	63.03	63.68	65.34	67.26	66.05	67.46	61.28
TiO ₂	0.459	0.79	0.528	0.451	0.51	0.39	0.68
Al ₂ O ₃	15.87	15.73	15.87	16	15.96	15.23	15.67
Fe ₂ O ₃	6.69	5.91	3.87	3.59	4.14	3.37	6.49
FeO	6.02	5.32	3.48	3.23	3.73	3.03	5.84
MnO	0.103	0.073	0.045	0.052	0.06	0.05	0.1
MgO	3.26	3.04	2.46	1.46	1.79	1.39	2.87
CaO	4.68	4.48	3.9	3.15	3.39	3.08	5.12
Na ₂ O	4.08	3.8	5.13	4.41	4.6	3.98	3.98
K ₂ O	1.37	1.78	1.75	2.98	2.46	3.49	2.68
P ₂ O ₅	0.22	0.22	0.23	0.13	0.14	0.1	0.16
Mg# ^c	49	50	56	45	46	45	47
Sc	13	13	8	6	7	6	13
Ba	221	363	365	488	634	780	576
Cs	1.7	3.4	2.1	6.4	6.5	2.9	19
Ga	21	23	22	21	20.9	20.6	21.6
Hf	2.4	5.2	4.1	5.1	4.9	4.2	5
Nb	6.3	9	5	8.3	8.7	6.9	9.5
Rb	53	95	73	145	110.9	130.7	148.2
Sr	580	594	1220	450	701.6	423.5	493.1
Ta	0.24	0.65	0.26	0.62	0.6	0.5	0.6
Th	0.72	2.71	3.11	12.5	7.4	8	7.8
U	0.35	0.55	1.87	5.65	1.7	2.5	3
V	57	88	69	44	48	49	101
Zr	87	189	160	173	182.7	137.8	190.9
Y	8.8	9	10.8	14	11.3	11.2	20.4
La	28.7	32.4	28	31.5	30.7	22.1	24.4
Ce	56.6	64.7	59	58.5	67.7	45.3	55.6
Pr	5.87	7.16	6.66	6.13	7.25	4.79	6.47
Nd	22.1	25.6	27.1	21.6	24.9	17.1	25.4
Sm	4.03	4.02	5.37	3.59	4.2	3	4.7
Eu	1.65	1.65	1.76	0.87	1.14	0.75	1.13
Gd	2.91	3.31	4.02	3.38	2.81	2.17	3.92
Tb	0.36	0.38	0.5	0.47	0.41	0.32	0.6
Dy	1.91	1.86	2.43	2.47	2.27	1.92	3.31
Ho	0.34	0.35	0.4	0.51	0.36	0.35	0.63
Er	0.86	0.95	0.98	1.51	0.95	0.99	1.87
Tm	0.114	0.12	0.126	0.217	0.15	0.16	0.29
Yb	0.77	0.74	0.85	1.35	1	1.02	1.72
Lu	0.111	0.114	0.124	0.213	0.15	0.16	0.29
Cu	40	30		15	5.1	29.8	32.3
Pb	9	7	10	20	4.2	2.6	4.5
Zn	115	74	44	44	51	35	45
Cr	71	91	68	36	27.37	7	88.95
Ni	46	54	40	33	19.7	8.7	19.7
La/Yb	37.3	43.8	32.9	23.3	30.7	21.7	14.2
(La/Yb) _N ^d	26.7	31.4	23.6	16.7	22	15.5	10.2
Sr/Y	66	66	113	32	62	38	24

TABLE I | Continued

Sample	114-MAV-02	131-MAV-02	124-APJ-03	262-APJ-03	299-MJV-03	21-MJV-06	1-MJV-08	2-MJV-08
Sample area	N-Turku	N-Turku	N-Turku	N-Turku	N-Turku	N-Turku	N-Turku	N-Turku
N-coordinate ^a	6742059	6733416	6746124	6722304	6732579	6748150	6721803	6724323
E-coordinate ^a	3261895	3256552	3219565	3216698	3246027	3245158	3228244	3235243
Rock type ^b	Ton	Ton	Ton	Ton	Ton	Ton	Charn	Ton
Laboratory	Acme	Acme	GTK	GTK	GTK	Acme	Acme	Acme
SiO ₂	64.34	66.02	69.5	68.2	70.3	65.17	62.99	64.08
TiO ₂	0.61	0.53	0.44	0.44	0.33	0.46	0.88	0.71
Al ₂ O ₃	14.77	15.19	15.9	15.5	15.7	16.44	14.97	15.86
Fe ₂ O ₃	5.63	4.04	2.96	3.34	2.78	4.66	6.67	5.72
FeO	5.07	3.64	2.67	3	2.5	4.19	6	5.15
MnO	0.11	0.06	0.03	0.06	0.04	0.05	0.08	0.06
MgO	2.57	2.17	1.12	1.8	1.07	1.79	3.49	2.23
CaO	3.96	3.76	3.2	3.2	2.62	2.88	4.31	4.19
Na ₂ O	3.07	4.69	4.86	5.21	4.78	5.13	3.43	3.94
K ₂ O	3.62	2.21	1.52	1.73	1.94	2.31	1.8	1.59
P ₂ O ₅	0.13	0.14	0.1	0.12	0.1	0.17	0.24	0.23
Mg# ^c	47	52	43	52	43	43	51	44
Sc	11	8	6.02	6.68	3.6	11	13	8
Ba	624	574	136	276	511	162.1	424	404
Cs	13.7	3.3	n.a	n.a	n.a	3.5	3.4	4.4
Ga	20.8	22.9	28	26	53	23.6	19.5	21.5
Hf	5.1	3.4	4.02	3.21	3.32	3.1	6	4.8
Nb	9.9	5.6	9.29	6.29	5.95	8.5	10.5	10.2
Rb	161.5	58.8	90	69.6	84.5	126.3	89.9	73.7
Sr	457.6	881.8	431	668	423	437.9	504.6	595.5
Ta	0.7	0.3	0.37	0.39	0.51	0.6	2.7	0.6
Th	10.9	5.6	1.23	1.39	5.77	20.7	7	3.1
U	3	2	0.73	0.7	3.28	2.6	1.8	2.2
V	90	63	38	62	34	61	100	75
Zr	180.5	134.1	171	141	141	101.2	208.8	174.1
Y	19.2	9.7	3.75	7.45	7.41	10.8	15.5	11.8
La	24.7	20.7	11.1	17.2	17.4	63.6	36.4	23.5
Ce	54.9	43.7	19.6	30.9	31.4	117.1	73.2	48.1
Pr	6.33	5	2.08	3.43	3.14	12.42	9.26	6.53
Nd	22.8	18.1	7.93	13.7	11.3	38	36.9	24.6
Sm	4.4	3.5	1.73	2.32	1.71	4.8	6.04	4.1
Eu	0.96	1.07	0.61	0.74	0.53	0.7	1.31	1.15
Gd	3.61	2.45	1.51	2.14	1.53	3.65	4.89	3.54
Tb	0.57	0.38	0.19	0.28	0.24	0.49	0.62	0.47
Dy	3.25	1.79	0.83	1.47	1.26	2.03	2.96	2.44
Ho	0.61	0.32	0.14	0.26	0.25	0.31	0.57	0.41
Er	1.79	0.86	0.23	0.66	0.67	0.66	1.56	1.2
Tm	0.27	0.13	0.1	0.1	0.1	0.1	0.22	0.18
Yb	1.78	0.79	0.25	0.53	0.72	0.46	1.48	1.06
Lu	0.27	0.12	0.1	0.1	0.1	0.08	0.21	0.16
Cu	14.1	24.4	4	108	25	5	47.3	14.4
Pb	13.2	1.5	21	15	30	4.2	2.2	1.8
Zn	164	45	67	49	49	96	51	64
Cr	47.9	54.74	10	66	28	47.9	123.2	54.7
Ni	20.5	29.9	21	41	20	27.6	72.4	28.1
La/Yb	13.9	26.2	44.4	32.5	24.2	138.3	24.6	22.2
(La/Yb) _N ^d	10	18.8	31.8	23.3	17.3	99.2	17.6	15.9
Sr/Y	24	91	115	90	57	41	33	50

TABLE I | Continued

Sample	38-MJV-07	25-MJV-08	32-MJV-08	26-MJV-07	27-MJV-07	28-MJV-07	33.1-MJV-07	47-MJV-07
Sample area	N-Turku	S-Turku	S-Turku	S-Turku	S-Turku	S-Turku	S-Turku	S-Turku
N-coordinate ^a	6721183	6686410	6684545	6691986	6691739	6688922	6709189	6707133
E-coordinate ^a	3194461	3201310	3212685	3182516	3187404	3189018	3264711	3288519
Rock type ^b	Grdr	Ton	Ton	Ton	Ton	Charn	Grdr	Ton
Laboratory	Acme	Acme						
SiO ₂	69.89	63.31	64.38	66.57	66.51	67.31	69.5	71.56
TiO ₂	0.3	0.78	0.69	0.5	0.6	0.53	0.46	0.28
Al ₂ O ₃	15.1	15.38	15.62	15.55	16.55	15.5	15.11	14.36
Fe ₂ O ₃	2.68	6.49	5.9	4.23	4.15	3.68	3.85	2.49
FeO	2.41	5.84	5.31	3.81	3.73	3.31	3.46	2.24
MnO	0.03	0.08	0.07	0.06	0.04	0.04	0.02	0.03
MgO	0.76	2.76	2.86	1.71	1.41	1.61	1.15	0.53
CaO	2.32	3.18	4.14	3.49	3.65	3.44	2.87	1.94
Na ₂ O	4.44	3.78	3.06	4.33	4.3	4.22	4.08	3.34
K ₂ O	2.56	2.76	2.11	2.72	1.94	2.77	2.01	4.24
P ₂ O ₅	0.089	0.17	0.2	0.126	0.128	0.13	0.105	0.087
Mg# ^c	36	46	49	44	40	46	37	30
Sc	4	10	12	7	6	7	6	3
Ba	437	241	596	536	496	571	190	793
Cs	1.8	1.6	5.8	6.4	2.5	2.2	2.9	2.3
Ga	20.2	22.9	19	21.4	24.2	21	24.3	17
Hf	3.6	6.3	6.9	4.6	6.7	3.8	6.2	5
Nb	4.9	27.3	12.1	9.3	8.6	8.3	13.8	7.8
Rb	82	155.3	158.9	100.3	96.6	82.6	131.7	134.2
Sr	692	233.2	393	547.9	546.6	556.4	297.5	220
Ta	0.3	0.9	0.7	0.7	0.8	0.4	1.3	0.3
Th	6	5	12.5	6.5	10.9	2	17.3	23.6
U	2.5	0.9	3.4	2.1	4.3	1.3	3.6	4.2
V	34	85	89	55	44	47	37	14
Zr	112.4	226.2	262.2	159.3	259.6	144.7	222.2	162.4
Y	10.6	13.1	17.9	9.4	10	6.7	7.5	6.2
La	15.6	31.3	30.8	23.3	35.5	18.9	48	37
Ce	30.7	61.9	64.4	43	64.6	36.1	88.9	69.7
Pr	3.7	7.33	7.79	4.96	7.16	4.16	9.78	7.87
Nd	13.6	29.2	28.1	19.3	26.8	15.8	34.5	24.8
Sm	2.67	4.7	4.98	3.19	4.24	2.6	4.63	4.16
Eu	0.68	0.86	1.19	0.89	1.05	0.83	0.87	0.73
Gd	2.37	4.27	4.07	2.68	3.33	2.04	2.96	2.78
Tb	0.38	0.55	0.61	0.37	0.46	0.29	0.41	0.37
Dy	2.18	2.57	3.3	1.8	2.17	1.28	1.76	1.35
Ho	0.37	0.45	0.6	0.31	0.35	0.24	0.25	0.25
Er	0.99	1.18	1.68	0.88	0.93	0.64	0.52	0.59
Tm	0.15	0.17	0.24	0.13	0.13	0.09	0.06	0.12
Yb	0.69	0.96	1.49	0.77	0.81	0.57	0.4	0.46
Lu	0.12	0.15	0.22	0.12	0.12	0.08	0.05	0.09
Cu	9.3	3.6	20.6	9.9	8.4	4.7	3.3	4.1
Pb	102.3	2.5	4.2	8	4	3.8	6.1	10.2
Zn	6386	109	53	57	71	51	75	42
Cr	13.7	89	130	34.2	<13.7	27.4	<13.7	<13.7
Ni	6.4	46.9	62	22.5	9.8	23.5	7.4	3.4
La/Yb	22.6	32.6	20.7	30.3	43.8	33.2	120	80.4
(La/Yb) _N ^d	16.2	23.4	14.83	21.7	31.4	23.8	86.1	57.7
Sr/Y	65	17.8	22	58	55	83	40	35

TABLE I | Continued

Sample	48-MJV-07	34-MJV-07	35-MJV-07	36.1-MJV-07	37-MJV-07	PERKALA	10-MJV-08
Sample area	S-Turku	S-Turku	S-Turku	S-Turku	S-Turku	S-Turku	S-Turku
N-coordinate ^a	6709163	6710101	6710342	6713461	6715115	6708833	6709224
E-coordinate ^a	3269961	3190861	3190980	3190204	3191364	3195538	3219184
Rock type ^b	Ton	Ton	Ton	Ton	Ton	Ton	Grdr
Laboratory	Acme	Acme	Acme	Acme	Acme	Acme	Acme
SiO ₂	63.4	68.28	64.62	61.98	70.8	69.05	69.72
TiO ₂	0.78	0.54	0.99	1.25	0.3	0.33	0.32
Al ₂ O ₃	16.53	15.53	16.23	18.06	15.58	14.7	15.37
Fe ₂ O ₃	5.66	4.2	5.49	5.16	2.59	3.54	3.3
FeO	5.09	3.78	4.94	4.64	2.33	3.19	2.97
MnO	0.07	0.02	0.05	0.06	0.03	0.04	0.02
MgO	2.49	1.04	1.56	1.79	0.82	1.76	1.08
CaO	4	2.71	3.78	5.49	2.31	2.84	2.75
Na ₂ O	3.3	4.04	3.81	3.52	4.72	4.13	4.64
K ₂ O	2.25	2.62	2.22	1.84	2.17	2.75	1.6
P ₂ O ₅	0.253	0.171	0.31	0.286	0.079	0.064	0.07
Mg# ^c	47	33	36	41	39	50	39
Sc	9	6	7	9	3	9	4
Ba	742	532	494	322	386	455	234
Cs	7.7	1.9	3.7	4.5	3.9	2.2	1.2
Ga	21	21.7	22.3	23.3	22	18.7	20
Hf	7.2	7.4	6.9	4.1	3.7	3.7	2.8
Nb	11.6	12	18.2	12.3	4.5	6.1	2.6
Rb	143.8	133.9	158.7	139.7	109.2	117.9	62.2
Sr	546.9	263.3	458.6	364.1	433.6	268.5	545.1
Ta	0.8	0.6	0.9	0.6	0.5	0.6	0.3
Th	14.7	11.4	11.4	4.7	7.3	8.2	1.6
U	2.5	3.1	2.8	4.3	3.2	1.8	0.9
V	63	45	58	110	27	45	33
Zr	277.8	283.5	295.1	146.6	127.4	124.9	94.1
Y	12.8	7.7	12.3	10.7	7.2	6	3
La	58.7	54.5	59.1	21.5	15	19	8.1
Ce	107.6	105.1	118.1	47.3	28.6	32.1	15.4
Pr	11.97	12.08	14.08	6.06	3.27	3.42	1.75
Nd	37	39.6	48.4	24.8	12.1	13.4	6.1
Sm	4.81	5.6	7.07	4.41	2.16	2.41	1.27
Eu	1.28	0.94	1.58	1.25	0.61	0.61	0.52
Gd	3.35	3.41	4.55	3.19	1.78	1.9	1.16
Tb	0.46	0.38	0.55	0.43	0.27	0.28	0.15
Dy	2.49	1.76	2.68	2.18	1.38	1.28	0.72
Ho	0.48	0.27	0.38	0.37	0.25	0.22	0.12
Er	1.2	0.65	1	1.13	0.73	0.6	0.27
Tm	0.2	0.09	0.15	0.14	0.11	0.09	0.05
Yb	1.05	0.54	0.86	0.75	0.56	0.54	0.28
Lu	0.16	0.08	0.13	0.13	0.1	0.08	0.03
Cu	17.8	5.6	10.1	5.1	2.4	9.2	3.1
Pb	4.6	4.2	5.5	3.5	3.8	4.6	1.6
Zn	90	91	99	75	55	62	51
Cr	47.9	20.5	13.7	<13.7	<13.7	102.6	27
Ni	21	6.5	11.8	5.5	6.7	15.7	17
La/Yb	55.9	100.9	68.7	28.7	26.8	35.2	28.9
(La/Yb) _N ^d	40.1	72.4	49.3	20.6	19.2	25.2	20.8
Sr/Y	43	34	37	34	60	45	182

^aFinnish national KJ coordinates; ^bTrond=trondhjemite, Ton=tonalite, Dr=diorite, Grdr=granodiorite, Cham=pyroxene-bearing;

^cMg#=Magnesium number= Molecular Mg/(Mg+Fe²⁺)x100; ^dChondrite normalized values; <value=Below given detection limit;

n.a.=not analyzed. Major elements in wt% and other elements in ppm

TABLE II U-Pb SIMS isotopic results from rocks of the Uusikaupunki area, SW Finland

Sample Uusikaupunki Trondhjemite (12MJV06; National coordinates N=6760530, E=3196380)																
Sample/Spot	Comment	[U] ppm	[Th] ppm	[Pb] ppm	Th/U measured	¹ f ₂₀₆ %	²³⁸ U ²⁰⁶ Pb	± %	²⁰⁷ Pb ²⁰⁶ Pb	± %	² Disc. % 2σ lim.	³ Disc. % conv.	²⁰⁷ Pb ²⁰⁶ Pb	±1σ	²⁰⁶ Pb ²³⁸ U	±1σ
n2394-18a		682	145	266	0.21	0.03	3.020	1.48	0.1142	0.36		-1.5	1867.6	6.5	1843.8	23.7
n2394-18b		498	81	191	0.16	0.04	3.030	1.58	0.1144	0.33		-2.0	1870.5	5.9	1838.5	25.3
n2394-18d		305	20	114	0.06	0.04	3.038	1.58	0.1152	0.37		-3.0	1882.9	6.6	1834.4	25.3
n2394-42a		752	112	286	0.15	0.54	3.047	1.48	0.1146	0.64		-2.7	1874.3	11.5	1829.5	23.6
n2394-44a		828	31	306	0.04	1.23	3.042	1.50	0.1135	0.64		-1.5	1856.8	11.5	1832.1	24.0
n2394-45a		727	121	278	0.17	0.02	3.033	1.48	0.1140	0.23		-1.7	1864.4	4.2	1836.9	23.7
n2394-50a		800	155	314	0.19	0.21	2.979	1.47	0.1139	0.23		0.21	1862.6	4.1	1866.0	23.9
n2394-61b-2		338	71	127	0.21	0.11	3.116	1.59	0.1139	0.36	-0.68	-4.2	1861.9	6.5	1794.3	25.0
n2394-64a		561	103	215	0.18	0.01	3.055	1.47	0.1141	0.27		-2.5	1865.8	4.9	1825.3	23.5
n2394-76a-2		615	112	242	0.18	0.04	2.972	1.49	0.1143	0.24		0.04	1869.2	4.2	1869.9	24.2
n2394-87a		851	125	333	0.15	0.01	2.958	1.47	0.1147	0.27		0.16	1874.4	4.8	1877.1	24.0
n2394-118a		381	28	147	0.07	0.04	2.943	1.47	0.1140	0.29		1.3	1864.2	5.3	1885.7	24.1
n2394-49a		1742	60	496	0.03	2.77	3.949	1.49	0.1134	0.56	-20.6	-24.1	1855.3	10.1	1455.0	19.4
n2394-58a	core	400	300	251	0.75	1.34	2.227	1.47	0.1816	0.39	-9.4	-12.4	2667.4	6.4	2390.7	29.5
n2394-58b	rim	730	110	247	0.15	4.80	3.515	1.47	0.1282	0.61	-21.5	-25.0	2072.9	10.7	1613.9	21.1
n2394-61a		303	49	140	0.16	0.32	2.524	4.13	0.1168	1.71	2.5	15.0	1908.2	30.5	2151.3	76.1
n2394-75a	core	1147	99	533	0.09	0.01	2.495	1.47	0.1351	0.15		0.44	2164.7	2.7	2172.7	27.2
n2394-76a		798	222	222	0.28	1.61	4.203	1.52	0.1132	0.84	-24.1	-28.5	1852.1	15.1	1375.8	18.8
n2394-85a		614	207	157	0.34	2.20	4.612	1.53	0.1134	0.53	-31.8	-35.0	1854.8	9.5	1265.0	17.6
n2394-85b		1820	41	758	0.02	0.38	2.690	1.49	0.1136	0.16	7.9	11.3	1857.5	2.8	2037.9	26.1
n2394-86a	core	962	276	420	0.29	0.02	2.750	1.47	0.1206	0.18		2.1	1964.7	3.3	1999.5	25.4
n2394-117a		529	157	176	0.30	1.41	3.460	1.74	0.1151	1.19	-8.6	-14.7	1881.4	21.2	1636.4	25.2
n2394-18c	rim	1276	19	472	0.01	0.08	3.020	1.51	0.1126	0.22		0.09	1842.5	4.0	1844.0	24.2
n2394-41a	rim	1274	128	516	0.10	0.41	2.820	1.47	0.1126	0.28	3.8	7.2	1842.0	5.0	1956.7	24.9
n2394-61b	rim	2203	62	730	0.03	0.41	3.379	1.50	0.1125	0.32	-7.4	-10.4	1840.3	5.8	1671.1	22.1
Sample Uusikaupunki Diorite (28MJV05; National coordinates N=678270, E=3197080)																
n2811-1a		338	208	142	0.62	0.05	3.033	1.31	0.1145	0.59		-2.1	1871.4	10.7	1836.9	20.9
n2811-7a		244	137	105	0.56	0.02	2.980	1.30	0.1147	0.36		-0.59	1874.8	6.4	1865.2	21.1
n2811-9a		263	113	108	0.43	0.04	3.019	1.30	0.1151	0.41		-2.3	1881.4	7.3	1844.2	20.9
n2811-10a		367	192	154	0.52	0.02	3.025	1.30	0.1146	0.33		-2.0	1873.7	5.9	1841.4	20.9
n2811-11a		170	88	72	0.52	0.12	2.950	1.30	0.1142	0.74		0.91	1867.2	13.3	1882.0	21.3
n2811-16a		446	247	191	0.55	0.03	2.990	1.31	0.1143	0.28		-0.53	1868.7	5.1	1860.2	21.2
n2811-17a		690	241	287	0.35	0.02	2.927	1.30	0.1153	0.27		0.58	1884.9	4.8	1894.4	21.4
n2811-19a		394	210	165	0.53	0.02	3.038	1.30	0.1143	0.29		-2.1	1869.0	5.3	1834.3	20.8
n2811-20a		443	236	190	0.53	0.03	2.929	1.31	0.1147	0.36		1.2	1874.5	6.5	1893.3	21.6
n2811-24a		255	143	110	0.56	0.01	2.982	1.30	0.1143	0.35		-0.28	1868.7	6.3	1864.2	21.1
n2811-30a		188	94	80	0.50	0.03	2.968	1.30	0.1147	0.41		-0.20	1875.4	7.4	1872.1	21.2

TABLE II | Continued

Sample/Spot	Comment	[U] ppm	[Th] ppm	[Pb] ppm	Th/U measured	¹ f ₂₀₆ %	²³⁸ U ²⁰⁶ Pb	± %	²⁰⁷ Pb ²⁰⁶ Pb	± %	² Disc. % 2σ lim.	³ Disc. % conv.	²⁰⁷ Pb ²⁰⁶ Pb	±1σ	²⁰⁶ Pb ²³⁸ U	±1σ
n2811-31a		470	281	207	0.60	0.04	2.904	1.31	0.1152	0.34		1.5	1882.6	6.2	1907.6	21.6
n2811-33a		457	170	190	0.37	0.05	2.915	1.31	0.1143	0.36		2.0	1869.4	6.4	1901.3	21.5
n2811-34a		245	129	105	0.53	0.02	2.920	1.32	0.1141	0.49		2.0	1865.9	8.8	1898.7	21.7
n2811-35a		313	176	131	0.56	0.01	3.009	1.31	0.1140	0.45		-0.89	1864.0	8.0	1849.5	21.1
n2811-38a		260	107	106	0.41	0.04	3.029	1.30	0.1139	0.45		-1.4	1862.6	8.0	1839.1	20.9
n2811-42a		380	200	160	0.53	0.04	2.974	1.30	0.1149	0.40		-0.60	1878.3	7.2	1868.5	21.1
n2811-45a		330	169	137	0.51	0.03	3.063	1.30	0.1147	0.33	-0.32	-3.3	1874.8	6.0	1821.4	20.7
n2811-53a		221	118	95	0.53	0.04	2.931	1.30	0.1132	0.46		2.6	1850.8	8.2	1892.1	21.4
n2811-55a		362	224	155	0.62	0.03	2.995	1.30	0.1148	0.38		-1.2	1876.2	6.8	1857.1	21.0
n2811-57a		260	131	108	0.51	0.02	3.046	1.30	0.1151	0.37	-0.07	-3.1	1881.0	6.7	1830.0	20.8
n2811-58a		725	336	300	0.46	0.02	3.030	1.30	0.1150	0.22		-2.5	1879.6	4.0	1838.5	20.8
n2811-61a		135	69	57	0.51	0.07	2.970	1.30	0.1131	0.77		1.4	1849.1	13.9	1871.0	21.2
n2811-63a		749	348	312	0.46	0.03	2.982	1.31	0.1148	0.35		-0.79	1877.1	6.3	1864.2	21.2
n2811-68a		161	77	68	0.48	0.05	2.969	1.30	0.1145	0.54		-0.06	1872.4	9.7	1871.4	21.2
n2811-72a		209	120	89	0.58	0.04	3.015	1.30	0.1146	0.48		-1.7	1874.3	8.6	1846.5	20.9
n2811-73a		331	179	143	0.54	0.02	2.951	1.30	0.1140	0.33		1.0	1864.7	5.9	1881.1	21.3
n2811-76a		512	351	228	0.68	0.03	2.944	1.30	0.1144	0.27		0.95	1869.8	4.9	1885.2	21.3
n2811-82a		408	169	167	0.41	0.03	3.026	1.30	0.1145	0.30		-1.9	1872.3	5.4	1840.7	20.9
n2811-84a		342	160	147	0.47	0.02	2.918	1.31	0.1148	0.36		1.4	1876.3	6.5	1899.6	21.6
n2811-87a		230	93	98	0.40	0.02	2.910	1.30	0.1142	0.42		2.3	1867.2	7.5	1904.4	21.5
n2811-88a		308	176	131	0.57	0.02	3.007	1.30	0.1153	0.34		-2.0	1883.8	6.1	1850.5	21.0
n2811-92a		387	201	167	0.52	0.02	2.929	1.30	0.1146	0.30		1.3	1873.3	5.5	1893.7	21.4
n2811-89a		287	155	126	0.54	0.02	2.891	1.30	0.1143	0.38		2.9	1868.3	6.9	1915.1	21.6
n2811-93a		234	132	99	0.56	0.04	3.007	1.30	0.1144	0.50		-1.3	1871.1	9.0	1850.6	21.0
n2811-99a		224	130	95	0.58	0.04	3.018	1.30	0.1132	0.45		-0.43	1851.8	8.0	1844.9	20.9
n2811-102a		254	132	108	0.52	0.02	2.978	1.31	0.1137	0.52		0.47	1858.8	9.4	1866.4	21.2
<i>n2811-95a</i>		330	176	148	0.53	0.02	2.837	1.30	0.1144	0.33	1.5	4.7	1870.8	6.0	1946.3	22.0
<i>n2811-69a</i>		4469	1989	2003	0.45	0.00	2.760	1.30	0.1150	0.13	4.2	7.0	1879.3	2.4	1992.9	22.4
<i>n2811-18a</i>		338	206	138	0.61	0.37	3.158	1.30	0.1148	0.67	-2.4	-6.3	1876.3	12.0	1773.2	20.2

Trondhjemite sample: analyses used for calculating the age of the zoned and prismatic zircons are marked in **bold**, those used for the rim age are mark in *italics*.

Diorite sample: analyses excluded from calculation are marked in *italics*. 1f₂₀₆% is percentage of common ²⁰⁶Pb in measured ²⁰⁶Pb, calculated from the ²⁰⁴Pb signal assuming a present-day Stacey and Kramers (1975) model. ²Disc. % 2σ is the degree of discordance of the ²⁰⁷Pb/²⁰⁶Pb and ²⁰⁶Pb/²³⁸U ages at the 2σ level estimated from the measured ²⁰⁴Pb. ³Disc. % conv. is the discordance in conventional concordia space. Age calculations use the routines of Ludwig (2003) and follow the decay constant recommendations of Steiger and Jäger (1977).